# Synthesis of functional polymers for application towards poly(ethylene) containing barrier materials

### Khadija Iqbal

Department of Chemical Engineering McGill University Montréal, Québec, Canada

April 2016

A thesis submitted to McGill University in partial fulfillment of the requirements of the degree of Master of Engineering

©Khadija Iqbal, 2016

#### **Abstract**

A primary amine functional monomer, IDBA (3-isopropenyl- $\alpha$ ,  $\alpha$ -dimethylbenzylamine) was synthesized with minimal purification steps, high yield (up to 76%) and good conversion (98%) from a cheap, commercially available precursor m-TMI (3-isopropenyl- $\alpha$ , $\alpha$ -dimethylbenzyl isocyanate). Amine functional polymers of IDBA, MA (methyl acrylate) and AN (acrylonitrile) were then synthesized using 2,2'-Azobis(2-methylpropionitrile (AIBN) as an initiator in dimethylformamide (DMF). These polymers were reacted with poly(ethylene) grafted with maleic anhydride (PE – MAn) in a miniature conical counter rotating twin screw extruder (Haake Minilab) at a 20 wt% of the amine functional polymer and 40 wt% of the poly(ethylene) loading at 140 °C. Scanning electron microscopy (for particle size), differential scanning calorimetry (for  $T_m$ ) and thermogravimetric analysis techniques (for  $T_g$ ) were used to characterize the properties of the polymers and blend. This blend was compared to a non – amine functional polymer blend with AMS ( $\alpha$  – methyl styrene) replacing IDBA in the formulation. The SEM results showed smaller particles and hence better blending of the amine – functional polymer with poly(ethylene). This promising blend could be used to improve the barrier material properties of poly(ethylene).

Furthermore, oxazoline functional styrene/acrylonitrile (SAO) polymers with sufficiently high conversions (59%) and low polydispersity  $M_w/M_n$  (1.32) were synthesized using nitroxide mediated polymerization (NMP) with NHS – BlocBuilder. It was demonstrated that NMP can be used to synthesize living and controlled oxazoline functional polymers. These polymers were thermally stabilized by removing the N-tert-butyl-N-[1-diethylphosphono-(2,2-dimethylpropyl) nitroxide] (SG1). Differential scanning calorimeter (for  $T_m$ ) and thermogravimetric analysis techniques (for  $T_g$ ) were used to characterize thermal properties of the polymers. The SAO polymers were then mixed with poly(ethylene) grafter with acrylic acid (PE – AA) in a 20 wt% loading at 112 °C using a technique called solvent casting. SEM results indicated insufficient mixing, which is likely due to the extremely low melting point of the PE – AA used. This suggested that further blending evaluation was necessary.

#### Abrégé

Un monomère d'IDBA (3 monomère,-isopropényl- α, α -dimethylbenzylamine) comportant un groupe amine primaire fonctionnel a été synthétisé avec peu d'étapes de purification, avec rendement (jusqu'à 76 %) et un taux de conversion (98 %) élevés grâce à un précurseur économique disponible commercialement, le *m*-TMI (3-isopropényl-α,α-dimethylbenzyl isocyanate). Des polymères d'IDBA, de MA (acrylate de méthyle) et d'acrylonitrile aminés ont ensuite été synthétisés dans le diméthylformamide (DMF) en utilisant l'AIBN comme initiateur. Ces polymères ont été réagis avec le poly(éthylène) couplé avec de l'anhydride maléique (PE - MA) dans une extrudeuse miniature conique avec contre-rotation (Haake Minilab) à 20% et de 40% (g/g) de chargement à 140 °C. Les propriétés des polymères et de ces mélanges ont été caractérisées par microscopie électronique à balayage (MEB, taille des particules), par calorimétrie différentielle à balayage (Tm) et par des techniques d'analyse thermogravimétrique (Tg). Ce mélange a été comparé à un mélange de polymères sans amine fonctionnel avec AMS (α - méthyl styrène). Des particules plus petites ont été observées par MEB dans le mélange avec des amines fonctionnelles, indiquant un meilleur mélange entre les deux phases. Ce mélange prometteur pourrait être utilisé pour améliorer les propriétés barrière du poly(éthylène).

En outre, des polymères styrène/acrylonitrile (SAO) avec des fonctions oxaline ont été synthétisés à l'aide de nitroxyde médiée polymérisation (NMP) avec NHS – BlocBuilder en obtenant des conversions suffisamment élevées (59%) et une faible polydispersité (Mw/Mn de 1.32). Il a été démontré que le NMP peut être utilisé pour synthétiser des polymères vivant et contrôlés, comportant des groupes fonctions d'oxazoline. Des polymères avec une plus grande stabilité thermique ont été obtenus en enlevant le N-tert-butyl-N-[1-diethylphosphono-(2,2-diméthylpropyle) nitroxyde] (SG1). Les propriétés thermiques des polymères on été caractérisées par calorimétrie différentielle à balayage (Tm) et des techniques d'analyse thermogravimétrique (Tg). Le polymères de SAO polymères ont été ensuite mélangées avec le poly(éthylène) greffé avec de l'acide acrylique (PE - AA) avec un chargement de 20% (g/g) à 112°C à l'aide d'une technique appelée le moulage de solvant. Les résultats de MEB ne correspondaient pas avec la proportion massique de 80%/20% (g/g). Une évaluation plus approfondie des mélanges sera donc nécessaire.

#### Acknowledgements

Firstly, I would like to express my sincere gratitude to my supervisor Prof. Milan Marić, for the continuous support of my studies and research, for being patient with me when nothing worked, for motivating me to achieve my potential, and for sharing some of his immense knowledge with me. His guidance helped me in all the time of research and writing of this thesis. I could not have imagined having a better supervisor and mentor for my Master's study.

I would also like to thank my fellow lab mates for the insightful comments and discussions but also for all the good memories we made. Especially thank Simon Kwan for training me on various equipment and always being there to lend a helpful hand. My office mate, Zohreh Mosaferi, thank you for all the laughs we shared. My summer students Brenden and David, thank you for your hard work and dedication. It was a pleasure working and learning together this past summer. I wish you all the best of luck in the future.

A big thank you to the Department of Chemistry for the use of the analytical equipment; Frederick Morin for NMR training and help, and Petr Fiurasek in the Centre for Self-Assembled Chemical Structures for his assistance with the FTIR, TGA and DSC.

Also a thank you to the Natural Sciences and Engineering Research Council of Canada, Imperial Oil Limited and the Department of Chemical Engineering at McGill University for funding the research.

Finally, I would like to thank my family for their unconditional love and support. I could not have done it without you all.

#### **Contribution of the Author**

The following thesis is based on two manuscripts, which will be submitted to "Macromolecular Materials and Engineering". I, Khadija Iqbal am the first author for both manuscripts. As a contribution to this manuscript, I have performed all monomer synthesis reactions for the primary amine. Some polymer synthesis reactions, modification, characterization, blending, morphology analysis and interpretation of the results were performed in collaboration with my summer students Brenden Moeun and David Zhang. I have written the manuscripts, which were revised and edited by my supervisor, Prof. Milan Marić.

#### List of Abbreviations and Symbols used

PE Poly(ethylene)

MA Methyl Acrylate

AN Acrylonitrile

STY Styrene

AMS  $\alpha$  – Methyl Styrene

*m*-TMI 3-isopropenyl- $\alpha$ , $\alpha$ -dimethylbenzyl isocyanate

IDBA 3-isopropenyl- α, α –dimethylbenzylamine

iPOx 2-isopropenyl-2-oxazoline

MMA Methyl Methacrylate

PMMA Poly(methyl methacrylate)

AIBN 2,2' -Azobis(2-methylpropionitrile)

MA/AN/IDBA Methyl acrylate/Acrylonitrile/IDBA terpolymer

MA/AN/AMS Methyl acrylate/Acrylonitrile/α-Methyl styrene terpolymer

DMF N, N-dimethylformamide

THF Tetrahydrofuran

NMP Nitroxide Mediated Polymerization

GPC Gel Permeation Chromatography

MALDI Matrix-assisted laser desorption/ionization

<sup>1</sup>H NMR Proton Nuclear Magnetic Resonance

FTIR Fourier Transform Infrared Spectroscopy

SEM Scanning Electron Microscopy

PE - MAn Maleic anhydride grafted poly(ethylene)

PE – AA Poly(ethylene) co – acrylic acid

CDCl<sub>3</sub> Deuterated chloroform

f Monomer feed mole ratio

F Polymer feed mole ratio

PDI Polydispersity index  $(M_w/M_n)$ 

 $M_n$  Number average molecular weight

M<sub>w</sub> Weight average molecular weight

 $\langle D \rangle_{\rm VS}$  Average particle size

## **Table of Contents**

Abstract	I
Abrégé	II
Acknowledgements	III
Contribution of the Author	IV
List of Abbreviations and Symbols used	V
GENERAL INTRODUCTION	1
I. Barrier Polymers	1
II. Methods of Polymerization	3
III. Polymer Blending	4
IV. Compatibilization	5
CHAPTER 1	7
1. Introduction	7
2. Research objectives	8
3. Synthesis of 3-isopropenyl-α, α-dimethylbenzylamine (IDBA) monomer	13
3.1. Materials	13
3.2. Experimental	14
3.2.1. Procedure I: Synthesis of IDBA via methyl urethane intermediate	14
3.2.2. Procedure II: Synthesis of IDBA via carbamate intermediate	16
3.2.3. Procedure III: Synthesis of amino-functional polymer	18
3.3. Results and Discussion	20
3.3.1. Procedure I	20
3.3.2. Procedure II	23
3.3.3. Procedure III	25
4. Compatibilization of MA/AN/IDBA and MA/AN/AMS with PE – MAn	28
4.1. Materials	28
4.2. Experimental	28
4.2.1. Investigating copolymerization behaviour of MA/IDBA and MA/AMS	28
4.2.2. Synthesis of MA/AN/IDBA and MA/AN/AMS with AIBN	30
4.2.3. Thermal Properties	31
4.2.4. Reactive Blending of MA/AN/IDBA and MA/AN/AMS terpolymer and PE $-$ MAn $\dots$	32
4.2.5. Sample preparation for microscopy	32
4.2.6. Image Analysis	33

4.2.7.	Characterization	33
4.3.1.	Investigating copolymerization behaviour of MA/IDBA and MA/AMS	36
4.3.2.	Thermal Stability of Polymers	46
4.3.3.	Reactive Blending of MA/AN/IDBA and MA/AN/AMS with PE – MAn	47
4.4. Co	nclusion	51
4.5. Fut	ure Work	52
CHAPTER 2		53
1. Introduc	tion	53
2. Research	h Objectives	55
3. Compati	ibilization of STY/AN/iPOx (SAO) with PE – AA	56
3.1. Ma	terials	56
3.2. Exp	perimental	57
3.2.1.	Synthesis of STY/AN/ iPOx (SAO) with AIBN	57
3.2.2.	Nitroxide Mediated Polymerization of STY/AN/iPOx (SAO) with NHS –	BlocBuilder58
3.2.4.	Removal of SG1 end group	60
3.2.6.	Solvent casting of SAO and Acrylic acid Grafted Poly(ethylene)	61
3.2.7.	Sample preparation for microscopy	62
3.2.8.	Image Analysis	62
3.2.9.	Characterization	62
3.3. Res	sults and Discussion	62
3.3.1.	Synthesis of SAO with AIBN	62
3.3.2. N	Nitroxide Mediated Polymerization of STY/AN/iPOx (SAO)	63
3.3.3.	Chain extension of STY/AN/iPOx polymer	68
3.3.5.	Solvent casting of SAO and Acrylic acid Grafted Poly(ethylene)	69
3.4. Con	nclusion	71
3.5. Fut	ure Work	71
GENERAL C	CONCLUSION	72
REFERENCI	FS	73

# **List of Figures**

Figure 1. Propagating reactions in a free radical copolymerization system [19]	10
Figure 2. Synthesis of methyl urethane from m-TMI precursor	14
Figure 3. Synthesis of IDBA from methyl urethane intermediate	15
Figure 4. Synthesis of IDBA via carbamate intermediate reaction scheme [26]	16
Figure 5. Synthesis of primary amine functional polymer using poly (methyl acrylate-m-TM	II) as
a precursor	18
Figure 6. FTIR spectra of methyl urethane (dotted line) and m-TMI (solid line) to indicate	
synthesis	21
Figure 7. <sup>1</sup> H NMR of methyl urethane intermediate in CDCl <sub>3</sub>	21
Figure 8. <sup>1</sup> H NMR of IDBA showing unreacted methyl urethane peaks at 3.5 ppm and 5.75	ppm
in CDCl3	23
Figure 9. <sup>1</sup> H NMR of IDBA synthesized via carbamate intermediate in CDCl <sub>3</sub>	24
Figure 10. FTIR spectra of m-TMI, carbamate and IDBA	24
Figure 11. (a) GPC plot (THF, 30°C) of MA/m-TMI synthesis reaction (b) Plot of ln[(1 - X)	-1]
(X = monomer conversion) versus time	26
Figure 12. FTIR spectra of amine functional polymer	26
Figure 13. <sup>1</sup> H NMR of amine functional polymer in CDCl <sub>3</sub>	27
Figure 14. a) General schematic of the PRS set up [27], b) Copolymerization reaction set up.	29
Figure 15. (A) Linear Mayo - Lewis plot for MA/IDBA copolymerization, (B) Extended Ke	len–
Tüdos (extended K–T) plot, (C) Kelen– Tüdos plot (K – T)	40
Figure 16. Linear Mayo – Lewis plot of MA and AMS copolymerization	44
Figure 17. (a) GPC plot (DMF, 50 °C) for MA/AN/IDBA terpolymer with initial molar feed	,
compositions $f_{MA,0} = 0.50$ and $f_{AN,0} = 0.40$ (b) Plot of $ln[(1 - X)^{-1}]$ (X = monomer conversion	n)
versus time for MA/AN/IDBA (c) GPC plot for MA/AN/AMS terpolymer with initial molar	feed
composition $f_{MA,0} = 0.50$ and $f_{AN,0} = 0.40$ (d)Plot of $ln[(1 - X)^{-1}]$ (X = monomer conversion)	
versus time for MA/AN/AMS.	46
Figure 18. SEM images of a) PE-MAn/MA/AN/IDBA (80/20) non-annealed, b) PE-	
MAn/MA/AN/IDBA (80/20), annealed at 130 °C for 18 hours, c) PE-MAn/MA/AN/AMS	
(80/20) non-annealed, d) PE-MAn/MA/AN/AMS (80/20), annealed at 130 °C for 18 hours	50
Figure 19. a) PE-MAn/MA/AN/IDBA (60/40) non-annealed, b) PE-MAn/MA/AN/IDBA	
(60/40), annealed at 130 °C for 18 hours, c) PE-MAn/MA/AN/AMS (60/40) non-annealed, of	(l:
PE-MAn/MA/AN/AMS (60/40), annealed at 130 °C for 18 hours	51
Figure 20. Structure of statistical STY/AN/iPOx (SAO) polymer	54
Figure 21. Dissociation of BlocBuilder, (b) Synthesis of succinimidyl ester terminated	
BlocBuilder (NHS – BlocBuilder) [39]	59
Figure 22. Structure of Sty/AN/iPOx (SAO) – SG1 terpolymer	61
Figure 23. Mn and PDI vs conversion plot of the NMP polymerization of Sty, An and iPOx is	n a)
$f_{STY} = 0.40$ , $f_{AN} = 0.50$ , $f_{iPOx} = 0.10$ monomer feed ratio, b) $f_{STY} = 0.50$ , $f_{AN} = 0.30$ , $f_{iPOx} = 0.50$	0.20

monomer feed ratio c) $f_{STY} = 0.50$ , $f_{AN} = 0.20$ , $f_{iPOx} = 0.30$ monomer feed ratio (3 hr reaction)
d) $f_{STY} = 0.50$ , $f_{AN} = 0.20$ , $f_{iPOx} = 0.30$ monomer feed ratio (24 hr reaction)
Figure 24. Plot of $ln[(1 - X) - 1]$ (X = monomer conversion) versus time a) $f_{STY} = 0.40$ , $f_{AN} =$
$0.50$ , $f_{iPOx} = 0.10$ monomer feed ratio, b) $f_{STY} = 0.50$ , $f_{AN} = 0.30$ , $f_{iPOx} = 0.20$ monomer feed
ratio c) $f_{STY} = 0.50$ , $f_{AN} = 0.20$ , $f_{iPOx} = 0.30$ monomer feed ratio (3 hr reaction) d) $f_{STY} = 0.50$ , $f_{iPOx} = 0.50$ , $f_{iPOx$
$AN = 0.20$ , $f_{iPOx} = 0.30$ monomer feed ratio (24 hr reaction)
Figure 25. GPC plot (THF, 40 °C), using PMMA standards, for SAO terpolymers with initial
$molar \ feed \ compositions \ a) \ f_{STY,0} = 0.40, \ f_{AN,0} = 0.50, \ f_{iPOx} = 0.10, \ b) \ f_{STY,0} = 0.50, \ f_{AN,0} = 0.30, \ d_{AN,0} = 0.00, \ d_{AN,0$
$f_{iPOx} = 0.20,  c)  f_{STY,0} = 0.50,  f_{AN,0} = 0.20,  f_{iPOx} = 0.30  (3hr  reaction),  d)  f_{STY,0} = 0.50,  f_{AN,0} = 0.20,  f_{AN,0} = 0.2$
$f_{iPOx} = 0.30 (24 \text{ hr reaction})$
Figure 26. GPC plot (THF, 40 °C), using PMMA standards, for SAO terpolymers as macro
initiators with initial molar feed compositions a) $f_{STY,0} = 0.40$ , $f_{AN,0} = 0.50$ , $f_{iPOx} = 0.10$ , b) $f_{STY,0} = 0.40$ , $f_{AN,0} = 0.50$ , $f_{iPOx} = 0.10$ , b) $f_{STY,0} = 0.40$ , $f_{AN,0} = 0.50$ , $f_{iPOx} = 0.10$ , b) $f_{STY,0} = 0.40$ , $f_{AN,0} = 0.50$ , $f_{iPOx} = 0.10$ , b) $f_{STY,0} = 0.40$ , $f_{AN,0} = 0.50$ , $f_{iPOx} = 0.10$ , b) $f_{STY,0} = 0.40$ , $f_{AN,0} = 0.50$ , $f_{iPOx} = 0.10$ , b) $f_{STY,0} = 0.40$ , $f_{AN,0} = 0.50$ , $f_{AN,0} = $
$= 0.50, f_{AN,0} = 0.30, f_{iPOx} = 0.20$
Figure 27. Reactive blending of Oxazoline and Carboxylic acid
Figure 28. SEM images of PE - AA /SAO (80/20), annealed at 130 °C for 6 hours70

### **List of Tables**

Table 1. Experimental conditions for the synthesis of IDBA	16
Table 2. Synthesis of IDBA via carbamate intermediate experimental data	18
Table 3. Copolymerization conditions and results for MA and IDBA	36
Table 4. Linear Mayo – Lewis equation parameters for IDBA and MA copolymerizations	37
Table 5. Non – Linear Mayo – Lewis parameters for IDBA and MA	38
Table 6. Parameters for the K-T method for MA and IDBA copolymerization	39
Table 7. Parameters for extended K-T method for MA and IDBA copolymerization	39
Table 8. Summary of reactivity ratios for MA and IDBA copolymerization	41
Table 9. Copolymerization conditions and results for MA and AMS	42
Table 10. Mayo – Lewis parameters for MA and AMS copolymerizations	43
Table 11. Non - linear or instantaneous Mayo - Lewis equation parameters for MA and AMS	S
copolymerization	
Table 12. Experimental conditions for the terpolymerizations of MA/AN/IDBA	45
Table 13. Experimental conditions for the terpolymerizations of MA/AN/AMS	46
Table 14. Thermal properties of MA/AN/IDBA polymers	47
Table 15. Thermal properties of MA/AN/AMS polymers	47
Table 16. Summary of blend microstructure for extruded blends and annealed blends	49
Table 17. Experimental data for the conventional free radical polymerization of STY/AN/iPC	
Table 18. Experimental data of NMP using STY/AN/iPOx	
Table 19. Thermal properties of SAO via NMP	69
Table 20. Summary of blend microstructure for extruded blends and annealed blends	71

#### GENERAL INTRODUCTION

#### I. Barrier Polymers

Traditional definitions of barrier polymers focus on oxygen permeability and water–vapor transmission rates. Simply put, barrier polymers are meant to separate a system from the surroundings – to allow no entry into the system or exit from the system or to preferentially allow some species to pass and others not to. All polymers are barrier polymers to some degree but different polymers are barriers for different applications. However, no polymer is a perfect barrier [1].

Substances/permeants can move through polymers or even into the polymers. The molecules of the substances collide with the polymer surface and then are dissolved into the polymer bulk. After this, the kinetic energy of the molecules drives their movement within the polymer bulk, jumping from vacancy to vacancy. The random diffusion causes a net distribution from a high concentration or partial pressure of the permeant molecules to a low concentration of permeant molecules along the gradient. After crossing the barrier polymer, the molecules move to the surface and enter the environment. Permeant movement is a physical process that has both a thermodynamic and a kinetic component. The permeant diffuses into the environment and the polymer according to thermodynamic rules of solution. The kinetic aspect is responsible for diffusion of the molecules. The net rate of movement is dependent on the speed of permeant movement and the availability of new vacancies in the polymer. **Equation 1** is an adaptation for films of *Fick's first law* [1]:

$$\frac{\Delta M_x}{\Delta t} = \frac{PA \, \Delta p_x}{L}$$
 (Equation 1)

 $\frac{\Delta M_x}{\Delta t}$  is the steady-state rate of permeation of permeant x through a polymer film, P is the permeability coefficient (commonly called the permeability), A is the area of the film,  $\Delta p_x$  is the

difference in pressure of the permeant on the two sides of the film, and L is the thickness of the film. The permeability is the product of the diffusion coefficient D and the solubility coefficient S as shown in **Equation 2**.

$$P = DS$$
 (Equation 2)

The diffusion coefficient (D), sometimes called the diffusivity, is the kinetic term that describes the speed of movement. The solubility coefficient (S), is the thermodynamic term that describes the amount of permeant molecules that will dissolve in the polymer. A polymer can have a low permeability because it has a low value of D or a low value of S, or both. A low value of D can result from either static or dynamic effects. Static effects include molecular packing in the amorphous phase, orientation, and the amount of crystallinity. A low value of S can observed when the permeant does not condense readily or does not interact strongly with the polymer. This can occur when there are no specific interactions, such as dipole-dipole interactions or hydrogen bonding, between the polymer and the permeant molecules or if the crystallinity is too high for the molecules to dissolve into the polymer. Lowering these two quantities and therefore the permeability of a polymer makes it a better barrier polymer [1]. One way to reduce the solubility coefficient is to decrease the interactions of the permeant molecules with the polymer. Polyethylene (PE) for example, is a hydrophobic polymer. Using polyethylene as a barrier polymer for gasoline or any other hydrocarbon would be ineffective as any non-polar compound can easily diffuse or flow out of the polymer. However, introducing polar segments into polyethylene (by blending with another polymer) would significantly decrease its permeability to non-polar compounds.

#### II. Methods of Polymerization

Polymerizations can be classified based on their underlying mechanism. Polymerizations in which polymer chains grow step-wise by reactions that can occur between any two molecular species are known as *step-growth polymerizations*. Polymerizations in which polymer chain grows only by reaction of monomers with a reactive end-group on the growing chain are known as *chain-growth polymerizations* (these usually require a reaction between monomer and initiator) [2].

This research was focused on a type of chain-growth polymerization called *radical polymerization*. This type of polymerization can be conventional *free radical polymerization* (FRP) or *controlled radical polymerization* (CRP) depending on the initiator used. FRP does not require stringent process conditions and can be used for (co)polymerization. However, the major limitation of FRP is poor control over some of the key parameters that would allow the preparation of well-defined polymers with controlled molecular weight, polydispersity, composition, chain architecture, and site-specific functionality. CRP provides such control, leading to an unprecedented opportunity in materials design, approaching the control of truly living polymerizations while largely maintaining the many advantages of FRP [3]. For example, block copolymers can be readily produced by CRP, and they can even be obtained in an emulsion/miniemulsion polymerization in aqueous media, a process not possible by living polymerizations like ionic polymerization.

There are broadly three types of controlled radical polymerizations: *nitroxide mediated* polymerization (NMP), atom transfer radical polymerization (ATRP) and reversible addition fragmentation chain transfer (RAFT). The basic principle underlying CRP is to suppress termination to the extent that it becomes insignificant by reversibly trapping and temporarily deactivating the chain radicals. This cycle of activation-deactivation is rapid. There are two

general strategies; reversible end capping of a chain radical or a rapid exchange of an end-capped radical with a free chain radical [2], [3].

End group functionalization in NMP and RAFT generally involves radical displacement/addition chemistry. In ATRP and iodine transfer radical polymerization, nucleophilic substitution and electrophilic addition are also possible. In all systems, essentially every (dormant) chain is capped with a protecting group. Dormant species are metastable in NMP and may be light sensitive in RAFT [3]. The most readily available, stable, and inexpensive groups forming dormant species are alkyl halides employed in ATRP [3]. However, ATRP also requires catalytic amounts of transition metal complexes that may need to be removed after the polymerization is completed. NMP is selected in this proposal, instead of RAFT and ATRP because it is easier to implement (only the unimolecular initiator/mediator is required – in this case using the nitroxide commercially known as BlocBuilder® (Arkema)) and it does not have the odour problems associated with thioester based chain transfer agents required with RAFT nor the discolouration issues associated with the presence of metallic ligands needed for ATRP [3, 4].

#### III. Polymer Blending

Polymer blends are mixtures of different homopolymers, copolymers, and terpolymers. The blends are classified as either miscible or immiscible; the former is defined as homogenous down to the molecular level, having negative free energy of mixing:  $\Delta G_m \approx \Delta H_m \leq 0$ , and a positive value of the second derivative;  $\frac{\partial^2 \Delta G_m}{\partial \phi^2} > 0$ , where  $\emptyset$  is the phase ratio (volume fraction of the dispersed phase).

Whether a mixture of two chemically dissimilar polymers is miscible or not depends on the thermodynamics of mixing [3]. According to the Gibbs free energy equation (**Equation 3**), for the

two polymers to blend, either the  $\Delta H$  of blending has to be negative or the  $\Delta S$  has to be positive. However, for an amorphous polymer with very long chains, the number of possible configurations is limited, so the  $\Delta H$  effect tends to dominate and the entropy is very low compared to small molecules. This presents a problem for polymer blending.

$$\Delta G = \Delta H - T \Delta S$$
 (Equation 3)

In order to achieve polymer to mixing, the first law of thermodynamics is applied. The first law states that a system always goes from a state of more energy to a state of less energy. So for two polymers to mix, they should have less energy when mixed than they do when separated. Thus, generally, for most polymer blends, the enthalpy of mixing dominates over entropic considerations.

Consequently, most polymer blends are immiscible and it is well known that the physical properties of these phase-separated polymers (such as toughness, flowability and weather resistance) are dictated by their morphology. Due to this, a variety of chemical and physical methods have been exploited to control the morphology of immiscible polymer mixtures. Most of the immiscible blends have poor interfacial adhesion and weak mechanical properties. To convert immiscible blends to useful polymeric products with the desired properties and stable morphologies, a third component called a compatibilizer can be used, which is miscible in both materials. The compatibilizer reduces the interfacial tension and suppresses coalescence of the dispersed phase [5].

#### IV. Compatibilization

Compatibilization is the process in which the interfacial properties of immiscible polymer blends are modified. The result is a reduction in interfacial tension, resulting in improved adhesion to

achieve the desired stable morphology. Compatibilization is accomplished either by adding a compatibilizer or by reactive processing.

- 1. Compatibilization by Addition of Pre-Made Copolymer: A block or graft copolymer is added as a third component. It is essential that the compatibilizer be designed to migrate to the interface and reduce interfacial tension. Thermodynamics requires that the added copolymer concentrates at the interface between the two homopolymers and is not wasted as micelles in either phase. The formation of micelles reduces the efficiency of the compatibilizer, and may lessen the mechanical performance of the blend. It could also be possible that the compatibilizer diffuses too slowly and does not reach the interface during the blending time allotted. Nowadays, only a few commercial alloys are prepared using the compatibilizer-addition method [6].
- 2. Reactive Compatibilization: Currently, the dominant method of compatibilization is based on a specific chemical reaction between two polymeric components during melt blending. The chemical reaction takes place in situ at the interface between two suitably functionalized homopolymers with complementary functional groups. The interfacial reaction creates the compatibilizer directly at the interface, avoiding the micellization and diffusion issues associated with pre-made copolymers that lead eventually to poor mechanical performance. Economically, reactive blending is attractive as the synthesis of pre-made copolymers with the proper characteristics could be prohibitive; while grafting or using inherent functionality (e.g. polyesters or polyamides typically have reactive residues such as acids, alcohols and amines at their chain ends) is accomplished readily. The conditions for reactive blending require that there is: (i) sufficient dispersive and distributive mixing to generate adequate interfacial area; (ii) presence of functionalities

capable of reacting across the interface; (iii) sufficiently fast reaction kinetics, making it possible to produce enough compatibilizing copolymer at the interface within the residence time of the processing unit; (iv) stability of the morphology. [6].

The chemistry behind the compatibilization process indicates that the probability of the two functional groups to react with each other in an extruder, during typical residence time, is low. In order for these groups to react, they need to be highly reactive and/or low molecular weight polymers may have to be used to increase concentration of end-groups. The majority of polymers that are functionalized have nucleophilic end-groups such as carboxylic acid, anhydride, amine or hydroxyl groups. These groups readily form covalent bonds with suitable electrophilic groups such as epoxide, oxazoline, isocyanate or carbodiimide, generating the desired copolymer [6]. The amine-anhydride functionalities are used in the first part of this thesis since this reaction has been characterized as being particularly effective in reactive blending [7, 8] and is used in commercial blends (e.g. rubber toughened nylon such as DuPont's Nylon ST) and the oxazoline – acid functionalities are used in the second part [9].

#### **CHAPTER 1**

#### 1. Introduction

The market for value-added commodity polymers such as polyethylene is lucrative and appealing as a wide variety of properties can be accessed by simple modification and blending. By blending polyethylene with other polymers, a diverse set of materials can be synthesized, possessing its own particular and advantageous qualities. In the scope of this investigation, a barrier polymer with grease resistance, oxygen barrier properties and tensile strength was to be synthesized through polyethylene blending with an appropriate dispersed phase polymer. This specific value-added

polyethylene will be used to make a better barrier material for hydrocarbon storage tanks by preventing leaks/diffusion.

Methyl acrylate (MA)/acrylonitrile (AN) copolymers were chosen here as the dispersed phase. Acrylonitrile in the copolymer offers excellent gas barrier properties (against oxygen and water vapor) as well as grease resistance [10, 11]. Methyl acrylate, on the other hand, provides the barrier material with high tensile strength and processability [12, 13]. However, due to the relatively polar nature of the MA/AN copolymer, it is immiscible with polyethylene and thus blending would not be very effective. To overcome this problem, compatibilization via reactive blending was investigated. The amine – anhydride reaction for compatibilization has been documented as the fastest and most effective in literature, and thus it was selected in this case [7]. In light of this, an amine functional group was needed on the MA/AN copolymer and an anhydride functional group on the polyethylene for reactive blending.

#### 2. Research objectives

There are several routes toward the development of amino-functional polymers but the goal of this project was to develop cost-effective and direct methods to obtain dispersed phase barrier polymers with controlled placement of amino-groups. The target was a terpolymer composed of acrylonitrile (AN), methylacrylate (MA) and a styrene derivative with the desired amine functional group. The choice of monomers was simple; AN provided the barrier properties, MA provided the processability (it is very difficult to process pure poly(acrylonitrile) and thus it is often copolymerized) and the styrenic derivative provided the amino functional group required for reactive compatibilization. The amine/anhydride reaction has been characterized as the most effective in polymer blending due to its rapid kinetics and thus the amine functional terpolymer

could be conveniently blended with commercially available polyethylene that is grafted with maleic anhydride [7, 14].

# A) Synthesis of cost effective styrene derivative with the desired primary amine functional group

Previous work with 4-aminostyrene has indicated that it can be incorporated into a polymer using free — radical polymerization [8]. However, such commercially available amine functional monomers (protected or unprotected) are generally expensive. (CAD 43\$/g of 4-aminostyrene [15] and CAD 145\$/g of N-tBOC-MAm [16]) and larger-scale synthesis requires cheaper functional monomers. The approach chosen was to first produce the amino-functional copolymer using a precursor monomer from easily available commercial sources. Such a monomer was obtained from suitable conversion in high yield from the isocyanate precursor, 3-isopropenyl- $\alpha$ , $\alpha$ -dimethylbenzyl isocyanate (m-TMI) [17]. The precursor isocyanate monomer was considerably cheaper than other amine-containing monomers (CAD \$0.452/1 g) [18]. The amino-functional monomer produced was called 3-isopropenyl- $\alpha$ ,  $\alpha$ -dimethylbenzylamine (IDBA).

#### B) Testing copolymerization behaviour

Before IDBA could be incorporated into a polymer, aspects of its copolymerization with MA/AN monomers had to be examined. First, it was necessary to establish that IDBA did not react unusually with other monomers in the presence of typical free radical initiators such as AIBN. Conventional free radical polymerizations of IDBA with methyl methacrylate (MMA) and styrene (STY), respectively, has been documented in literature [17]. The copolymerization of IDBA with methyl acrylate (MA) was carried out with varying compositions under the same conditions, to establish copolymerization behaviour. When a copolymer is formed, there are two types of radicals that can form the growing chain. There is radical M1• from monomer 1 and radical M2• from monomer 2. Each of these radicals can attack either monomer, hence four propagating reactions

are possible as shown in **Figure 1**. The rate of homopolymerization of monomer 1  $(k_{11})$  refers to the rate of addition of monomer 1 to the M1• terminal radical. The rate of copolymerization of monomer 1  $(k_{12})$  refers to the addition of monomer 2 to the terminal radical M1. The reactivity ratio of monomer 1 therefore is the ratio between the rate of homopolymerization and copolymerization i.e.  $r_1 = k_{11}/k_{12}$  which essentially states the preference for monomer 1 to add to itself relative to monomer 2. The same principle applies for the reactivity ratio of monomer 2,  $r_2 =$  $k_{21}/k_{22}$  [19]. The instantaneous form of the Mayo – Lewis equation (**Equation 4**) was then used to evaluate the monomer reactivity ratios for these copolymerizations. The Mayo-Lewis equation is important in copolymerizations in that it relates the instantaneous monomer composition to the copolymer composition. The linearized form of the Mayo – Lewis equation was used to fit the data and obtain estimates for the reactivity ratios (**Equation 5**). The Kelen–Tüdos method (K - T) and extended Kelen-Tüdos method (extended K-T) were also used to calculate reactivity ratios [20, 21] since the extended K – T method can be used for higher conversions because it considers the effects of conversion. The K-T equation is shown in **Equation 6** and the same equation is used for extended K - T method, however the parameters are calculated depending on polymer conversion [22]. Once the ratios are determined, we may predict the composition of the polymer formed at any conversion from any mixture of that monomer pair [23]. The copolymerization and calculation of reactivity ratios of MA and AN has already been done and documented in literature using conventional free – radical polymerization with AIBN initiator [24].

$$M_1^* + M_1 \xrightarrow{k_{11}} M_1^*$$

$$M_1^* + M_2 \xrightarrow{k_{12}} M_2^*$$

$$M_2^* + M_1 \xrightarrow{k_{21}} M_1^*$$

$$M_2^* + M_2 \xrightarrow{k_{22}} M_2^*$$

**Figure 1.** Propagating reactions in a free radical copolymerization system [19]

$$\mathbf{F_1} = \mathbf{1} - \mathbf{F_2} = \frac{\mathbf{r_1 f_1^2 + f_1 f_2}}{\mathbf{r_1 f_1^2 + 2 f_1 f_2 + \mathbf{r_2 f_2^2}}}$$
 (Equation 4)

$$\frac{f(1-F)}{F} = r_2 - r_1 \frac{f^2}{F} \qquad \text{(Equation 5)}$$

 $F_1$  = Mole fraction of monomer 1 in polymer,  $F_2$  = Mole fraction of monomer 2 in polymer,  $F = F_1/F_2$   $f_1$  = Mole fraction of monomer 1 in initial feed,  $f_2$  = mole fraction of monomer 2 in initial feed,  $f = f_1/f_2$  $r_1$  = reactivity ratio of monomer 1,  $r_2$  = reactivity ratio of monomer 2

$$\eta = (\mathbf{r}_1 + \frac{\mathbf{r}_2}{\alpha})\xi - \frac{\mathbf{r}_2}{\alpha}$$
 (Equation 6)

 $\eta = G/(\alpha + H)$ ,  $\xi = H/(\alpha + H)$  and  $\alpha = (H_{min}H_{max})^{1/2}$ . The intercepts at  $\xi = 1$  and at  $\xi = 0$  of the plot of  $\eta$  against  $\xi$  gives  $r_1$  and  $r_2/\alpha$ , respectively.  $H_{min}$  and  $H_{max}$  are the lowest and highest values of H, respectively G and H are parameters for the K - T equation calculated as follows; G = F(f - 1)/f,  $H = F^2/f$  for the K - T method

G and H are calculated differently for the extended K-T method: G=(f-1)/Z,  $H=f/Z^2$  and  $Z=log(1-\xi_1)/log(1-\xi_2)$   $\xi_2=w(\mu+F)/(\mu+F)$  and  $\xi_2=\xi_1(f/F)$ ,  $w=polymer\ conversion$ ,  $\mu=molecular\ weight\ ratio\ of\ monomers$ 

The copolymerization of AMS with methyl acrylate (MA) was also carried out with the same initial monomer compositions and conditions as IDBA to calculate the reactivity ratio of AMS and compare the amine – functional styrene derivative (IDBA) to the non – functional styrene derivative (AMS). This way, the effect of the addition of an amine group (keeping all conditions constant) could be analyzed using reactive and non-reactive analogs. Since the goal was to obtain inexpensive amino–functional polymers, traditional free radical polymerization was used (we did not initially focus on trying to obtain co/terpolymers with complex microstructures). The first step in understanding how to place IDBA in a polymer chain was to examine its copolymerization reaction kinetics and determine how well it is incorporated into the copolymer chain.

#### C) <u>Terpolymerization</u>

The targeted amino-functional polymer was a terpolymer consisting of acrylonitrile (AN), methylacrylate (MA) and IDBA using traditional free radical polymerization techniques. IDBA was used in moderate levels (< 20 mol% in the feed) since excessive concentration of amine

functional groups was not necessary for reactive compatibilization. As we were targeting MA/AN copolymers for barrier applications, it was important to be aware that the acrylonitrile loading had to be relatively high, and this is why monomer feeds were restricted to a minimum composition of 50 mol% acrylonitrile in all cases. However, the maximum composition of 80 mol% acrylonitrile in the feed was set because poly(acrylonitrile) has a high melting point, high melt viscosity and is thermally unstable, and hence high acrylonitrile loading is problematic [10]. A series of initial monomer compositions were tested to observe their incorporation into the copolymer as this would influence the microstructure which would affect compatibilization and the properties of the copolymer. Initially, target molecular weights were kept low (10 - 20 kg/mol) to facilitate characterization and to minimize side reactions that become more dominant when higher molecular weights are targeted.

#### D) Reactive Blending

The amine – functional co/terpolymer was blended with maleic anhydride grafted PE (PE - MAn) via reactive extrusion. The effectiveness of the amine functionality in the terpolymers in the reactive blends was assessed by comparison with the non-reactive analog (PE - MAn with non-functional MA/AN copolymer). The blend morphologies were characterized to determine the level of compatibilization achieved, as witnessed by the dispersed phase particle size (i.e. coalescence was prevented by reactive compatibilization, which should result in smaller dispersed phase sizes). Further, morphological stability was tested by thermal annealing.

#### 3. Synthesis of 3-isopropenyl-α, α-dimethylbenzylamine (IDBA) monomer

#### 3.1. Materials

All compounds used as received unless otherwise stated. 3-Isopropenyl-α,α-dimethylbenzyl isocyanate (m-TMI, 95%, containing ≤200 ppm BHT as inhibitor), ethylene glycol butyl ether (butyl cellosolve,  $\geq 99\%$ ), dichloromethane (DCM,  $\geq 99.8\%$ ), dibutyltin dilaurate (DBTL, 95%), monoethanol amine ( $\geq$ 98%), ethylene diamine ( $\geq$ 99%), ethanol (96%), chloroform-d (99.8 atom % D) and 2,2'-Azobis(2-methylpropionitrile) (AIBN, 99%) were purchased from Sigma–Aldrich. Methyl acrylate (MA, 99%, containing ≤100 ppm monomethyl ether hydroquinone as inhibitor) was also purchased from Sigma-Aldrich and purified by passing through a column of basic alumina (Brockmann, Type 1, 150 mesh) mixed with 5% calcium hydride (90-95%, reagent grade), then sealed with a head of nitrogen and stored in a refrigerator until needed. N, Ndimethylformamide (DMF, 99.8%), tetrahydrofuran (THF, 99.9%), methanol (99.8%), 1, 2dichloroethane (≥99%), acetone (99.5 %), anhydrous ethyl ether (≥99 %) and anhydrous magnesium sulfate (certified) were purchased from Fisher and used as received. Anhydrous sodium sulfate (≥99.0%) was purchased from EMD BioSciences Inc. Potassium hydroxide (85%) was purchased from Acros Organics and used as received. Chloroform-d (CDCl<sub>3</sub>, 99.8 atom %) was purchased from Cambridge Isotope Laboratories. Hydrochloric acid (37%, 12 M) was purchased from ACP chemicals and diluted with water to get dilute hydrochloric acid (5%, 1 M). Maleic anhydride grafted linear low density poly(ethylene) (PE – MAn) (1.70 wt% grafted maleic anhydride) with a melt flow index (MFI) of 1.5 g (10 min)<sup>-1</sup> at 190 °C, density of 0.91g ml<sup>-1</sup>, melting point of 123°C (with the trade name Orevac 18302N) and a glass transition temperature of -42 °C was obtained from Arkema and used as received.

#### 3.2. Experimental

#### 3.2.1. Procedure I: Synthesis of IDBA via methyl urethane intermediate

#### A) Synthesis of methyl urethane

$$\begin{array}{c} \text{CH}_3 \\ \text{H}_2\text{C} = \overset{\text{C}}{\text{C}} \\ \text{H}_3\text{C} \\ \text{NCO} \\ \text{M} - \text{TMI} \end{array} \qquad \begin{array}{c} \text{CH}_3 \\ \text{H}_2\text{C} = \overset{\text{C}}{\text{C}} \\ \text{H}_3\text{C} \\ \text{H}_3\text{C} \\ \text{Methyl Urethane} \end{array}$$

Figure 2. Synthesis of methyl urethane from m-TMI precursor

A 50 mL three-neck round bottom glass flask equipped with a magnetic stir bar, reflux condenser, thermal well and pressure-equalizing addition funnel was used. The condenser was connected to an ethylene glycol/water mixture recirculating chiller (set at 4 ° C) and attached to the central neck of the flask to prevent the evaporation of the mixture components. The condenser was capped with a rubber septum containing an exhaust needle to relieve any pressure build up during the reaction. The flask was set inside a heating mantle and placed on a magnetic stirrer. A thermocouple was situated inside the thermal well, inserted in the second neck of the flask, and connected to a temperature controller. The reactant m-TMI (17.30 g) and the catalyst dibutyltin dilaurate (0.8 g) were added to the flask through the addition funnel. The methanol (2.77 g) was then added drop wise to the flask through the addition funnel, with stirring, over the course of about 30 minutes. The slow addition was necessary to control the exothermic reaction of the methanol with the reaction mixture. The reaction between the methanol and m-TMI is shown in Figure 2. A maximum exothermic increase of 20 °C was observed. The flask was allowed to cool to room temperature. Once the reaction mixture was well mixed, the pressure addition funnel was replaced with a rubber septum to seal the flask and the reaction mixture was heated at 60 °C under reflux

for 4 hours. A sample of the final mixture was taken and analyzed using Fourier transform infrared spectroscopy (FTIR). The infrared spectrum showed that the isocyanate peak (N=C=O), absorbance around 2700 cm<sup>-1</sup>, was no longer present. This confirmed that all the m-TMI had reacted. The reaction mixture was then transferred to a beaker and allowed to cool to room temperature, forming a white solid consisting of the methyl urethane intermediate. This solid was left to dry in the fume hood overnight. The final yield was 10.62 g of methyl urethane (53% yield).

#### B) Synthesis of IDBA

$$\begin{array}{c} \text{CH}_3 \\ \text{H}_2\text{C} = \overset{\bullet}{\text{C}} \\ \\ \text{CH}_3 \\ \\ \text{H}_3\text{C} \\ \\ \text{H}_3\text{C} \\ \\ \text{H}_3\text{C} \\ \\ \text{H}_3\text{C} \\ \\ \text{O} \\ \\ \text{Methyl Urethane} \\ \end{array}$$

Figure 3. Synthesis of IDBA from methyl urethane intermediate

The dried methyl urethane (10.62 g) was then dissolved in butyl cellosolve (10.7 g) solvent and this solution was once again transferred to a three neck round 50 mL round bottom flask equipped with a thermal well, reflux condenser and magnetic stir bar. A solution of potassium hydroxide (4.25 g, 1.7 times molar excess of methyl urethane) in butyl cellosolve (18.5 g) was added to the reaction mixture and it was allowed to react under reflux for 4 hours at a temperature of 60 °C. The reaction is shown in **Figure 3**. The mixture was then allowed to cool to room temperature and added to a beaker containing 60 mL of deionized water and 100 mL of 1,2-dichloroethane. The beaker was left to stir at room temperature for 12 hours, then brine was added to facilitate separation of the aqueous and organic layers and the contents were transferred to a separatory funnel. The organic layer was isolated, washed with water (2 x 200 mL), and then dried with anhydrous sodium sulfate. The dichloroethane was removed under reduced pressure using a

rotatory evaporator and the residue was subjected to vacuum distillation to separate the product and unreacted methyl urethane. This however proved ineffective due to the similar boiling points of the methyl urethane and dimethyl benzyl amine. The final yield of 3-isopropenyl- $\alpha$ , $\alpha$ -dimethylbenzylamine (IDBA) monomer was 6.54 g (43.6% yield). Thus, experiments were carried out at various conditions (stoichiometric ratio, temperature) to get higher yield and conversion as shown in **Table 1**.

Table 1. Experimental conditions for the synthesis of IDBA

Exp	Catalyst DBTL	Reaction	Urethane:KOH	Temp	Time	Separation	Yield (%)
No.	(g)	solvent	mole ratio	(°C)	( <b>h</b> )	solvent	
1	0.80	Butyl	1:1.7	60	4	1,2-Dichloroethane	Urethane: 53.0
		Cellosolve					IDBA: 43.6
2	1.69	Butyl	1:2	100	4	Dichloromethane	Urethane: 86.7
		Cellosolve				and Toluene	IDBA: 50.4
3	0.80	Acetone	1:1	60	24	Dichloromethane	Urethane: 86.5
							IDBA: 65.3
4	1.69	Butyl	1:1.7	60	24	1,2-Dichloroethane	Urethane: 76.4
		Cellosolve					IDBA: 81.4

#### 3.2.2. Procedure II: Synthesis of IDBA via carbamate intermediate

Figure 4. Synthesis of IDBA via carbamate intermediate reaction scheme [26]

A 100 mL three neck round bottom flask equipped with a thermal well and magnetic stir bar was charged with monoethanol amine (24.28 g, 397.5 mmol, 2 times molar excess compared to m-TMI used) and ethanol (~ 64.0 g, the solvent is added in a 1:1 ratio with the reaction mixture) and placed on a magnetic stirrer. A thermocouple was inserted in the thermal well and attached to a temperature controller. The other two necks of the flask were sealed with rubber septa. Over the course of 3 hours, m-TMI (40.0 g, 198.7 mmol) was added drop wise to the flask, using a syringe, with vigorous stirring at room temperature. The reaction is shown in **Figure 4**. This slow addition prevented a highly exothermic reaction. The temperature of the reaction mixture was allowed to subside for 15 – 20 minutes after which a sample was taken for FTIR analysis. The infrared spectra showed no isocyanate (N=C=O) absorbance peak around 2700 cm<sup>-1</sup>. Then the reaction mixture was added to a beaker equipped with a magnetic stir bar, containing anhydrous ethyl ether (30 mL) and dilute hydrochloric acid (20 mL, 1M ~ 5%). The mixture was left to stir at room temperature for 12 hours on a magnetic stirrer. Then the organic layer (ethyl ether) was isolated using a separatory funnel and washed with water (2 x 200 mL). The resultant material was dried with anhydrous sodium sulfate and left to dry in the fume hood for 24 hours. The carbamate (37.8 g, 144. 3 mmol) was transferred to a 50 mL three-neck round bottom glass flask equipped with a magnetic stir bar, reflux condenser, thermal well and vacuum distillation column. The condenser was connected to an ethylene glycol/water mixture recirculating chiller, set at 2 ° C, and attached to the central neck of the flask to prevent the evaporation of the mixture components. The condenser was capped with a rubber septum containing an exhaust needle to relieve any pressure build up during the reaction. The flask was set inside a heating mantle and placed on a magnetic stirrer. A thermocouple was situated inside the thermal well, inserted in the second neck of the flask, and connected to a temperature controller. The carbamate was heated at 120 °C for 24 hours

under reflux and simultaneous vacuum distillation was conducted at 80-100 mbar to push the equilibrium from the carbamate to the IDBA product by constant removal of the product as it is formed. The IDBA was washed with deionized water/5% water in sodium chloride to remove water-soluble impurities. The compound was then dried in a vacuum oven at 50 °C for 3 hours. The final yield of 3-isopropenyl- $\alpha$ , $\alpha$ -dimethylbenzylamine (IDBA) monomer was 18.7 g (73.9 % yield). The data for the experiments carried out is summarized in **Table 2**.

Table 2. Synthesis of	IDBA via carbama	ate intermediate ex	sperimental data
-----------------------	------------------	---------------------	------------------

	Solvent	Reactant 1	Reactant 2	Temp (°C)	Time (h)	Final product	Yield (%)
Exp 1(a)	Ethanol	Monoethanol	m - TMI	20	3	Carbamate	76.1
		amine					
Exp 1(b)	None	Carbamate	None	120	24	IDBA	76.3
Exp 2(a)	Ethanol	Monoethanol	m - TMI	20	3	Carbamate	72.6
		amine					
Exp 2(b)	None	Carbamate	None	120	24	IDBA	73.9

#### 3.2.3. Procedure III: Synthesis of amino-functional polymer

Figure 5. Synthesis of primary amine functional polymer using poly (methyl acrylate-m-TMI) as a precursor

#### A) Synthesis of poly(methyl acrylate-m-TMI) with AIBN

A conventional free-radical statistical copolymerization of MA/m-TMI, with the initial molar composition,  $f_{MA, 0} = 0.95$ , in 50wt% N, N dimethylformamide (DMF) was conducted at 70 ° C for

300 minutes. The polymerization was performed in a 25 mL three-neck round bottom glass flask equipped with a magnetic stir bar, condenser, and thermal well. The flask was set inside a heating mantle and placed on a magnetic stirrer. The central neck was connected to a condenser and capped with a rubber septum with a needle to relieve pressure applied by the nitrogen purge throughout the reaction. A thermocouple was connected to a controller and inserted into the second neck of the flask. The initiator (AIBN, 0.11 g, 0.7 mmol), and the stirrer were added via the third neck of the flask, which was then sealed with a rubber septum. Previously purified MA (5.688 g, 66.1 mmol), m-TMI (0.700 g, 3.5 mmol), and DMF (6.388 g, 87.5 mmol) were each injected into the flask via syringe. As stirring began and the monomers were well mixed, the chilling unit using a glycol/water mixture that is connected to the condenser was set to 4 °C. A nitrogen flow was introduced to purge the solution for 30 min. The reactor was then heated to 70 °C while maintaining the purge. The reaction was left for 300 minutes, after which the mixture was allowed to cool to room temperature. The final polymer was precipitated in a methanol and water mixture, vacuum filtered, and then dried for 120 minutes in a vacuum oven at 50 °C. The target number average molecular weight  $(M_n, target)$  at complete conversion, calculated by the mass of monomer relative to the moles of initiator, was set to 9.5 kg/mol. The final yield of the copolymer after 300 minutes was 2.3 g (48% conversion of monomers based on NMR analysis) with number-average molecular weight  $M_n = 3.5$  kg/mol and polydispersity index  $M_w/M_n = 3.43$  determined by gel permeation chromatography (GPC) calibrated relative to linear PMMA standards in THF at 40 °C. The MA molar composition of the copolymer using NMR analysis was  $F_{MA} = 0.949$ .

#### B) Functional group modification of isocyanate to primary amine

The MA/m-TMI copolymer was dissolved in DMF (37.9, 51.9 mmol) in a 125 mL single-neck glass round bottom flask equipped with a magnetic stir bar. The flask was sealed with a rubber

septum and fitted with a needle to relieve the purge. The mixture was purged with a flow of nitrogen for 30 minutes, then the purge and vent needles were both removed from the flask. Ethylenediamine (6.37 mL, 27 times molar excess) was added to the flask by syringe and was allowed to stir at room temperature for 300 minutes. The reaction taking place is shown in **Figure** 5. A precipitate could be seen after 30 minutes of stirring. Once the reaction was complete, the mixture was washed twice with deionized water and then washed with brine. The mixture was then dried using magnesium sulphate, filtered, and dried under vacuum. The remaining polymer was dissolved in THF, precipitated in hexanes and vacuum filtered. It was left in a vacuum oven overnight at 50 °C. The disappearance of the isocyanate peaks around 2200 cm<sup>-1</sup> using FTIR indicated reaction from the isocyanate to the amine.

#### 3.3. Results and Discussion

#### 3.3.1. Procedure I

FTIR spectroscopy was used to confirm the disappearance of the *m*-TMI isocyanate peak (around 2500 cm<sup>-1</sup>) and appearance of a carbonyl peak (around 1700 cm<sup>-1</sup>), as the reaction progressed, confirming the presence of the methyl urethane intermediate as shown in **Figure 6**. The structure of methyl urethane was further confirmed using <sup>1</sup>H NMR as shown in **Figure 7**.

The structure of the final product, IDBA, was confirmed with <sup>1</sup> H NMR as shown in **Figure 8**. Gravimetric conversion based on <sup>1</sup> H NMR, from methyl urethane to IDBA, was found to be 50% but could not be accurately determined due to butyl cellosolve and dichloroethane impurities in Experiment 1 from **Table 1**.

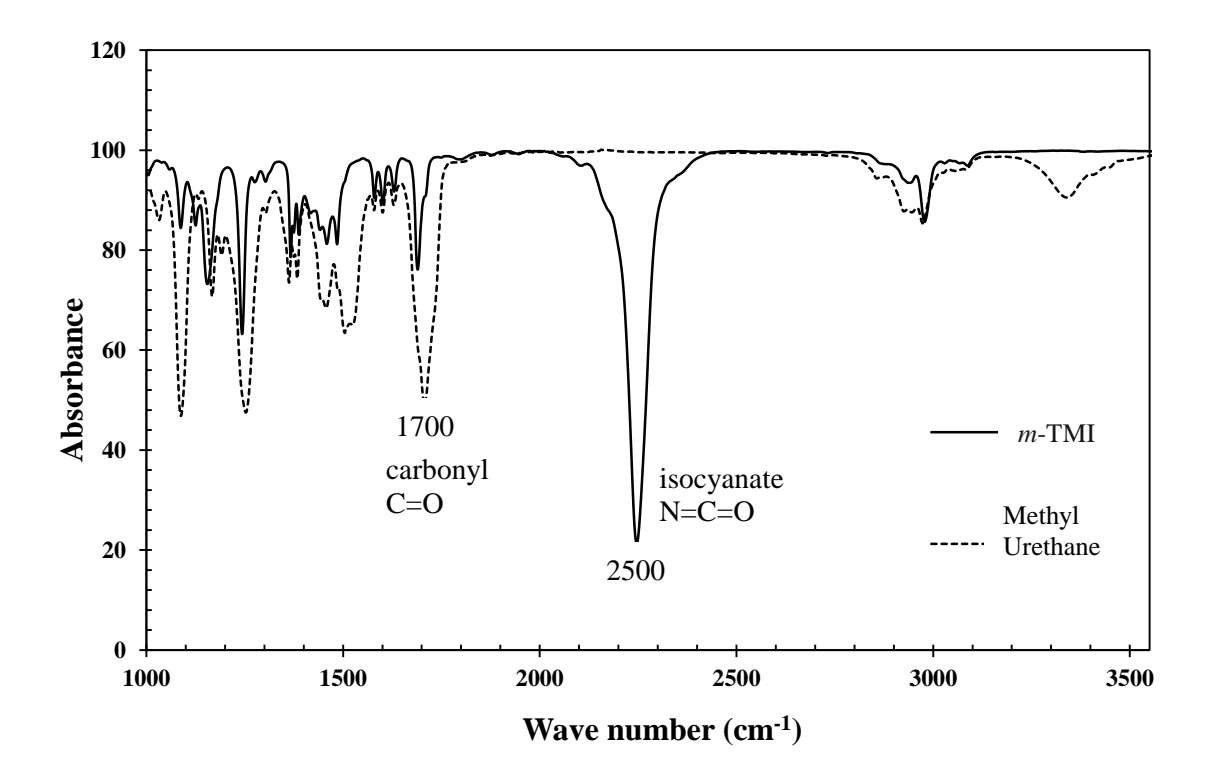


Figure 6. FTIR spectra of methyl urethane (dotted line) and m-TMI (solid line) to indicate synthesis

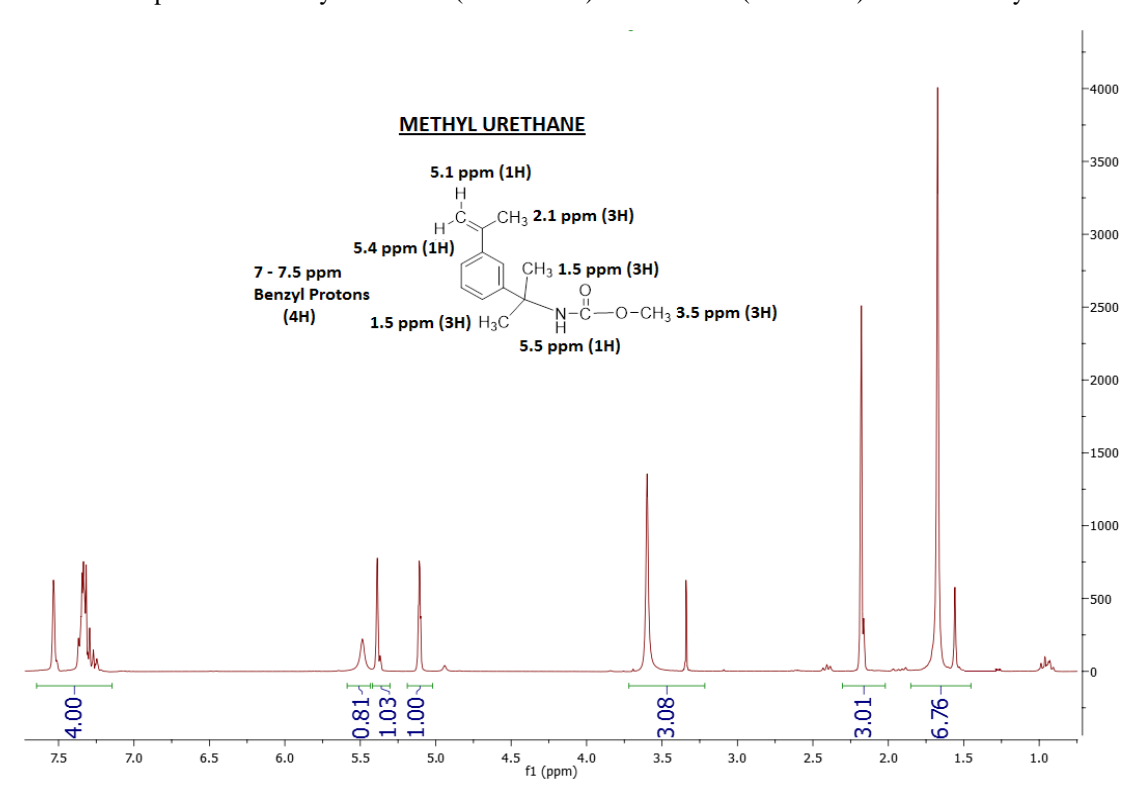


Figure 7. <sup>1</sup>H NMR of methyl urethane intermediate in CDCl<sub>3</sub>

In experiment 2 (from **Table 1**), dichloroethane was replaced with dichloromethane to enable better purification. Dichloromethane was chosen because it does not form an azeotrope with water during separation, unlike dichloroethane, and it also more volatile. The butyl cellosolve impurity however, still proved to be difficult to remove, so a more volatile solvent was used. The gravimetric conversion from methyl urethane to IDBA was again found to be 50% but could not be accurately determined due to the solvent (butyl cellosolve) impurity.

In Experiment 3 (from **Table 1**), butyl cellosolve was replaced with acetone, which has a comparatively lower boiling point. Conversion from the methyl urethane intermediate to IDBA was confirmed to be 50% through NMR analysis. However due to the low boiling point of acetone, the temperature was lowered to 60 ° C, and the reflux was maintained for 24 hours to ensure sufficient conversion. Once the conversion was confirmed in Experiments 1-3, in Experiment 4 (from **Table 1**), the 24 hour reflux was repeated with butyl cellusolve as the solvent and a higher yield was obtained.

In conclusions, the butyl cellosolve solvent led to higher initial product yield but product purification was problematic. Extensive purification steps had to be carried out with repeated vacuum distillation and it was very difficult to separate the methyl urethane intermediate from IDBA as shown by the <sup>1</sup>H NMR in **Figure 8**. This greatly reduced the final yield of purified product. Our results did not agree with those presented by Trumbo *et al* [17]. Perhaps they were able to remove the butyl cellusolve more effectively using a Kugelrohr apparatus.

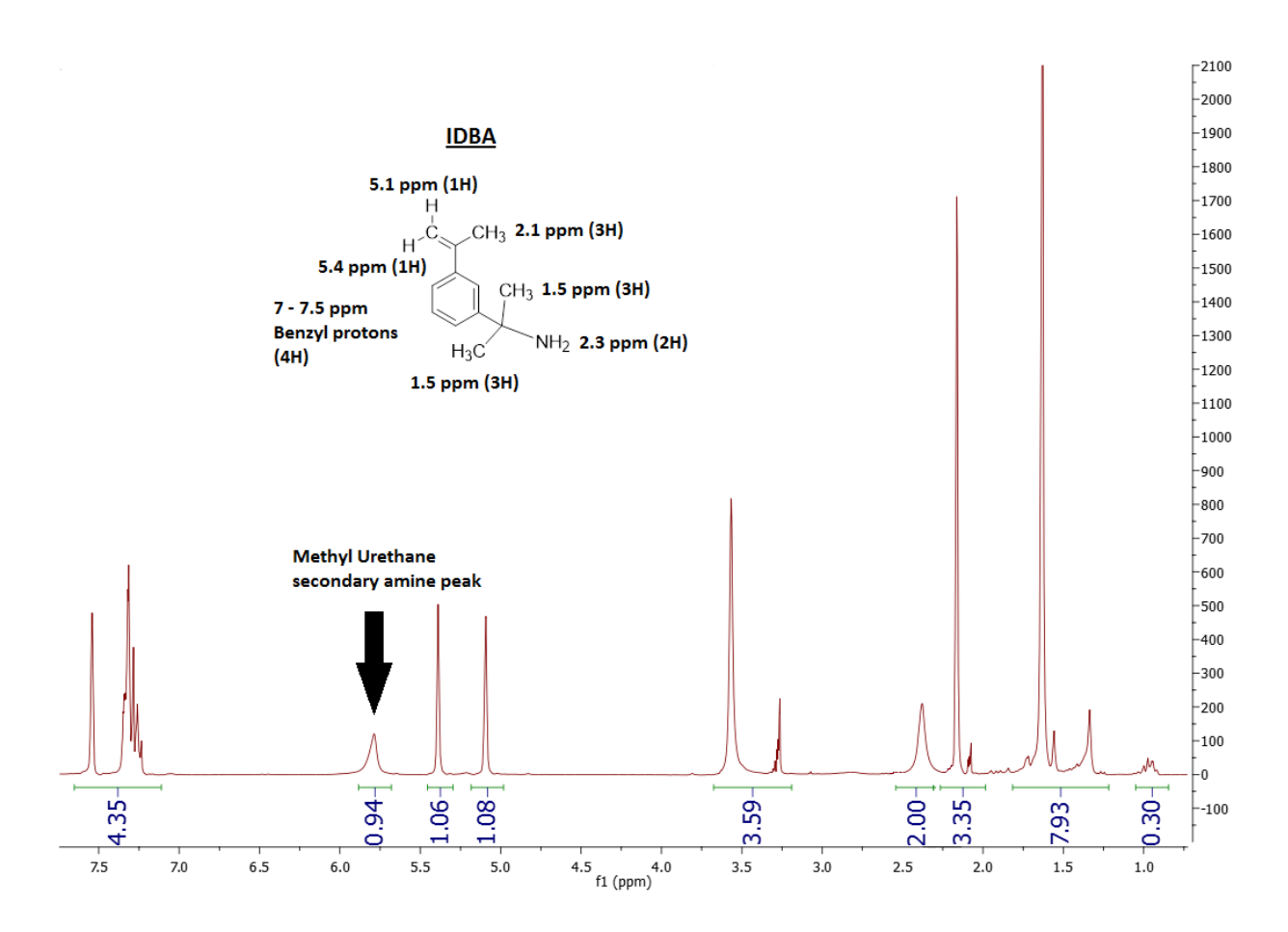


Figure 8. <sup>1</sup>H NMR of IDBA showing unreacted methyl urethane peaks at 3.5 ppm and 5.75 ppm in CDCl<sub>3</sub>

#### 3.3.2. Procedure II

This procedure (adapted from a patent by Charles *et al.* [26]) aimed to react an isocyanate with an alkanolamine to form a carbamate reaction product which was then thermally decomposed to form a primary amine product (IDBA) as shown in **Figure 4**. The equilibrium of the decomposition reaction is known to predominantly favour the carbamate rather than the amine product [26]. As a result, it was necessary to continuously remove the resultant amine product as it is formed via vacuum distillation.

The final structure of the IDBA was confirmed using <sup>1</sup>H NMR as shown in **Figure 9**. Conversion based on <sup>1</sup>H NMR from carbamate to IDBA was found to be 98%.

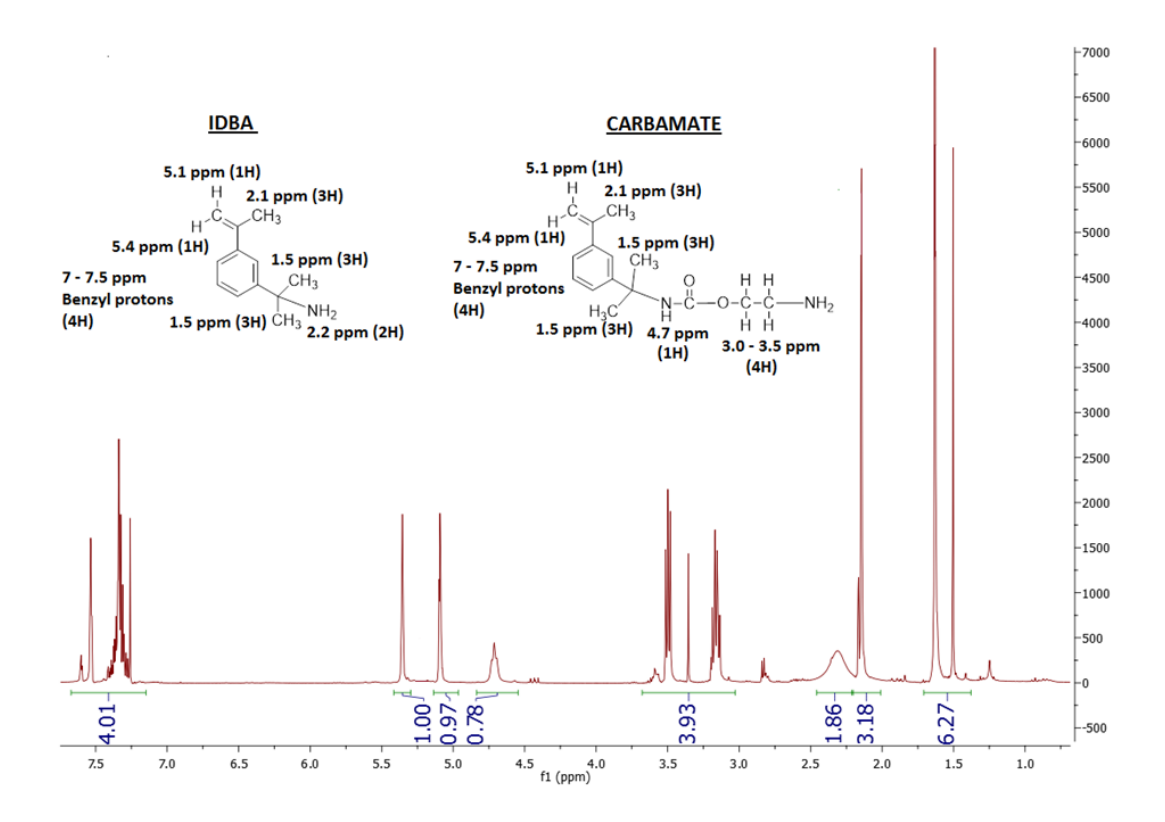


Figure 9. <sup>1</sup>H NMR of IDBA synthesized via carbamate intermediate in CDCl<sub>3</sub>

The progression of the reaction to convert *m*-TMI to the carbamate was confirmed using FTIR spectrometry. The peaks used to identify the compounds were the isocyanate peak in *m*-TMI (2200 cm<sup>-1</sup>), the carbonyl peak in the carbamate (1700 cm<sup>-1</sup>) and the primary amine peak in the IDBA (3300 cm<sup>-1</sup>) as shown in **Figure 10**.

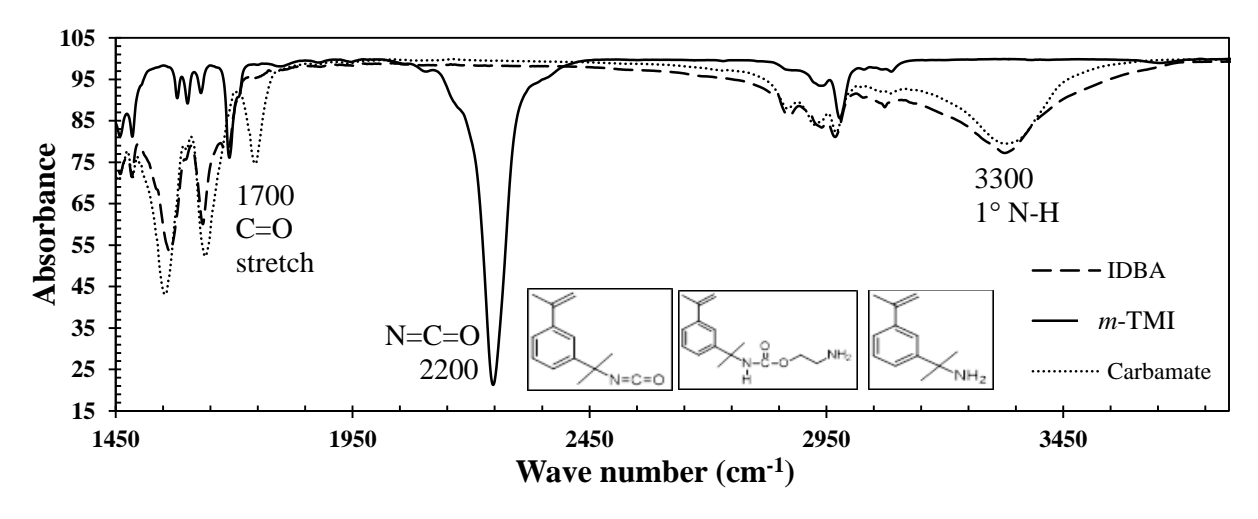


Figure 10. FTIR spectra of m-TMI, carbamate intermediate and IDBA

Procedure II has minimal purification steps, high yield and good conversion. Charles et al. [26] were able to get yields up to about 50% with this procedure. The yield is affected by the choice and amount of alcohol and amine used. In our procedure, we were able to get yields up to about 76% using ethanol and monoethanol amine. The monoethanol amine was used in a 2 times molar excess of the m-TMI precursor. The final yield was also influenced by the extraction process using ethyl ether and dilute hydrochloric acid. The ethyl ether organic layer dissolves the carbamate intermediate and leads to its separation from the water soluble impurities. In our procedure, the extraction was carried out for a period of 24 hours allowing a greater amount of intermediate to be dissolved in the organic layer hence, giving us a greater yield of final product. However, one of the most essential steps to getting a high yield was the continuous removal of IDBA product as it was formed via vacuum distillation. This procedure is a significant improvement on procedure I. Unlike procedure I, there are minimum purification steps since the decomposition of the carbamate to IDBA requires no solvent whereas, for methyl urethane, butyl cellosolve was used (which was difficult to separate). Procedure I also required the use of strong base such as KOH as a catalyst. This was not necessary in Procedure II. This procedure can be used as a cost – effective method to make primary amine functional moieties.

#### 3.3.3. Procedure III

The MA/*m*-TMI co-polymer was characterized using <sup>1</sup>H NMR, FTIR and GPC. The GPC plot in **Figure 11** shows the results of the free-radical co-polymerization.

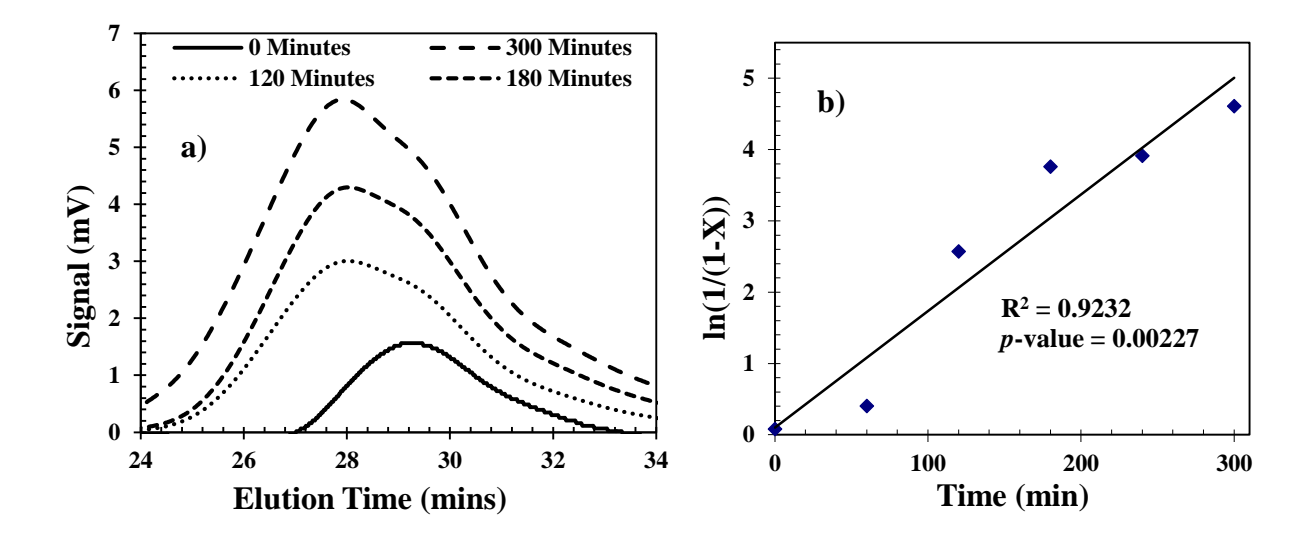


Figure 11. (a) GPC plot (THF,  $40^{\circ}$ C) of MA/m-TMI ( $F_{MA} = 0.95$ ) synthesis reaction (b) Plot of ln[(1 - X)-1] (X = monomer conversion) versus time

Subsequently, the MA/*m*-TMI co-polymer was reacted with excess ethylene diamine to form a primary amine functional polymer. The appearance of primary amine groups was detected using FTIR. The peak at 2200 cm<sup>-1</sup> due to the isocyanate in *m*-TMI disappeared and a primary amine peak at 3300 cm<sup>-1</sup> appeared, confirming that the reaction was successful, as shown in **Figure 12**. The presence of the amine functionality was further confirmed using <sup>1</sup> H NMR as shown in **Figure 13**.

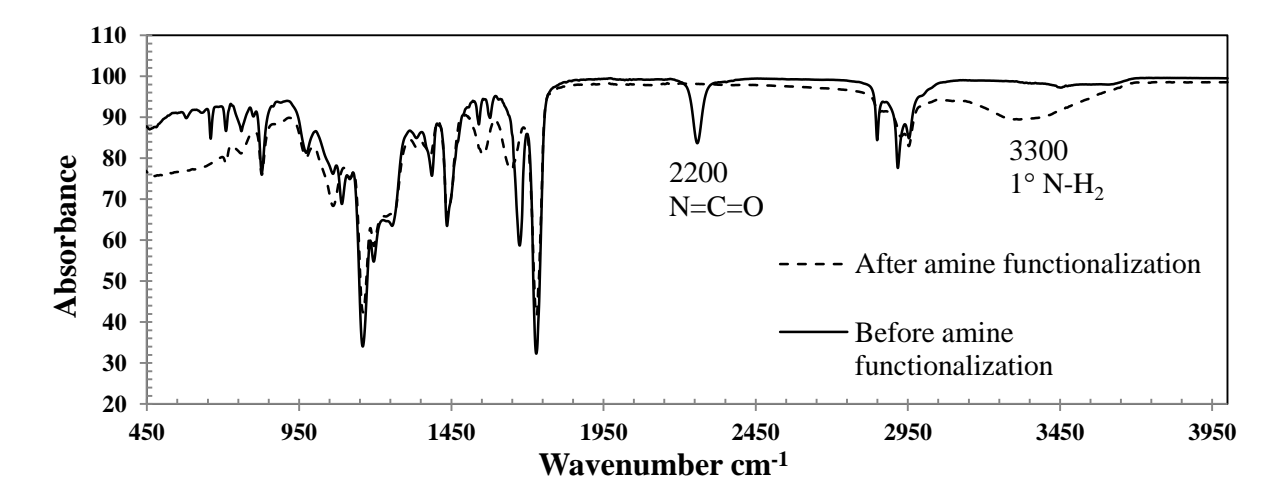


Figure 12. FTIR spectra of amine functional polymer

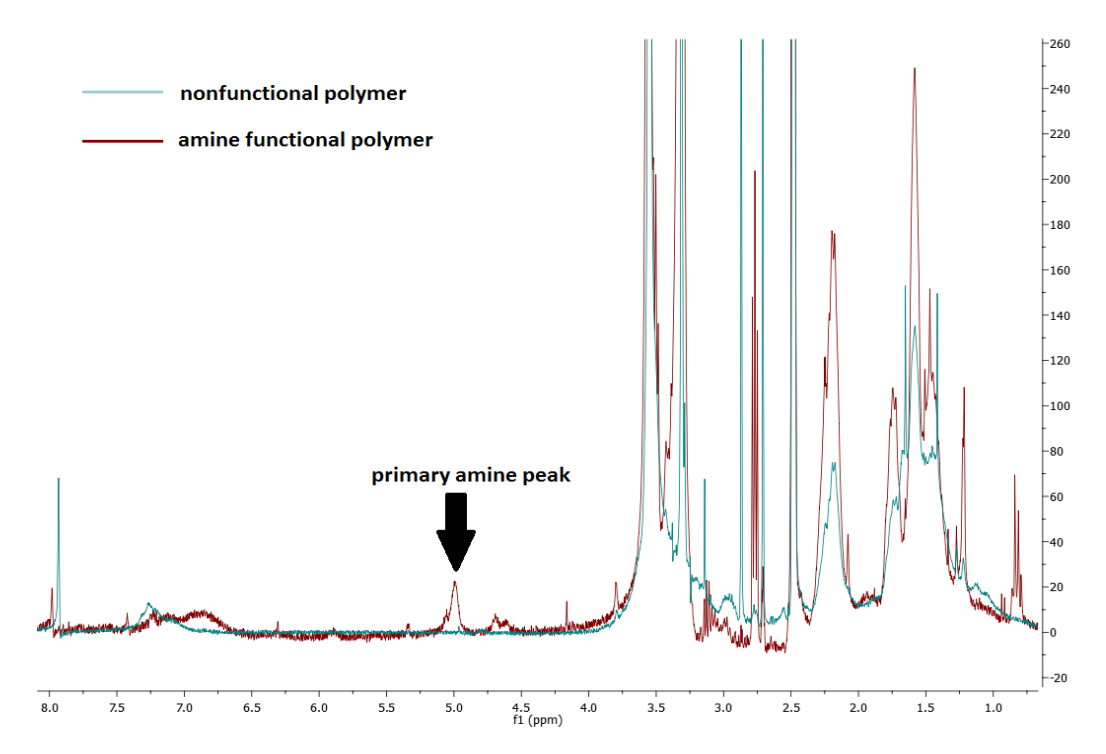


Figure 13. <sup>1</sup>H NMR of amine functional polymer in CDCl<sub>3</sub>

### 3.4. Conclusion

In this chapter, an amine-functional monomer, using a cheap isocyanate precursor was successfully synthesized in a cost – effective manner using procedure II. This amine-functional monomer was to be eventually incorporated in a terpolymer.

The *m*-TMI precursor was converted to a carbamate intermediate, and then thermally decomposed to form amino-functional IDBA. This procedure required few purification steps and high yields were obtained compared to procedure I. Also, methyl urethane intermediate to final product (IDBA) conversion was confirmed to be 50% through <sup>1</sup>H NMR analysis in procedure I whereas, for procedure II, the carbamate intermediate to IDBA conversion was found to be 98%. The final product was confirmed using <sup>1</sup>H NMR and FTIR spectroscopy. Procedure III was also documented as an alternative to synthesize amine-functional polymers directly from the isocyanate functional polymer.

# 4. Compatibilization of MA/AN/IDBA and MA/AN/AMS with PE – MAn

#### 4.1. Materials

Acrylonitrile (AN, ≥99%, contains 35-45 ppm monomethyl ether hydroquinone as inhibitor), Methyl acrylate (MA, 99%, containing ≤100 ppm monomethyl ether hydroquinone as inhibitor) and α-Methyl styrene (AMS, 99%, contains 15 ppm p-*tert*-butylcatechol as inhibitor) were purchased from Sigma-Aldrich and purified by passing through a column of basic alumina (Brockmann, Type 1, 150 mesh) mixed with 5% calcium hydride (90−95%, reagent grade), then sealed with a head of nitrogen and stored in a refrigerator until needed. *N*, *N*-dimethylformamide (DMF, 99.8%) and tetrahydrofuran (THF, 99.9%) were purchased from Fisher and used as received. 2,2′-Azobis(2-methylpropionitrile) (AIBN, 99%) was purchased from Sigma–Aldrich and used as received. Chloroform-d (CDCl<sub>3</sub>, 99.8 atom %) was purchased from Cambridge Isotope Laboratories and used as received. Dimethyl sulfoxide-d<sub>6</sub> (DMSO-d<sub>6</sub>, 99.9 atom %) was purchased from Sigma – Aldrich and used as received. Maleic anhydride grafted linear low density poly(ethylene) (PE – MA) with the trade name Orevac 18302N was obtained from Arkema and used as received.

# 4.2. Experimental

# 4.2.1. Investigating copolymerization behaviour of MA/IDBA and MA/AMS

A conventional free-radical polymerization, of MA-IDBA, with the initial molar composition,  $f_{MA,0} = 0.95$ ,  $f_{IDBA,0} = 0.05$ , in 50wt% N, N dimethylformamide (DMF) was carried out. The polymerization was performed in a Personal Reaction Station (PRS), purchased from KEM Scientific, Inc. The 20 mL glass tubes were equipped with magnetic stir bars. The internal electric heater was used to supply the heat (the heater has a temperature limit of 130 °C) [27]. The PRS temperature controller was connected to the PRS reactor. The condenser was connected to the

chilling/unit as a source of cooling. The gas inlet was connected to a nitrogen gas cylinder. The set up for the PRS is shown in **Figure 14**. The initiator (AIBN, 0.11 g, 0.7 mmol), and the stirrer were added via the third neck of the flask, which was then sealed with a rubber septum. Previously purified MA (8.40 g, 97.6 mmol), IDBA (0.90 g, 5.1 mmol) and DMF (9.30 g, 127.2 mmol) were each injected into the flask via syringe. As stirring began and the monomers were well mixed, the chilling unit using a glycol/water mixture that is connected to the condenser was set to 4 °C. A nitrogen flow was introduced to purge the solution for 30 min. The reactor was then heated to 70 °C while maintaining the purge. The reaction was left for the designated reaction time, after which the mixture was allowed to cool to room temperature. The final polymer was precipitated in methanol and water, decanted, and then dried for 120 minutes in a vacuum oven at 50 °C. The number average molecular weight  $M_n = 22.5$  kg/mol and polydispersity index  $M_w/M_n = 2.13$ (determined by gel permeation chromatography (GPC) calibrated relative to linear PMMA standards in DMF at 50 °C). A few drops of phenyl isocyanate were added to the vial before being introduced into the GPC column, to prevent the amine groups from attaching to the column. The MA and IDBA molar composition of the copolymer were  $F_{MA} = 0.96$  and  $F_{IDBA} = 0.04$ . They were calculated by <sup>1</sup>H NMR analysis (300 MHz, CDCl<sub>3</sub>, δ): 3.6 (s, 3H, O-CH<sub>3</sub>), 1.2-2 (m, 2H, backbone CH<sub>2</sub>). The same procedure was repeated for MA-AMS to make a non-functional copolymer for comparison with the amine functional IDBA terpolymer. Different molar compositions were also performed for functional and non – functional copolymers.

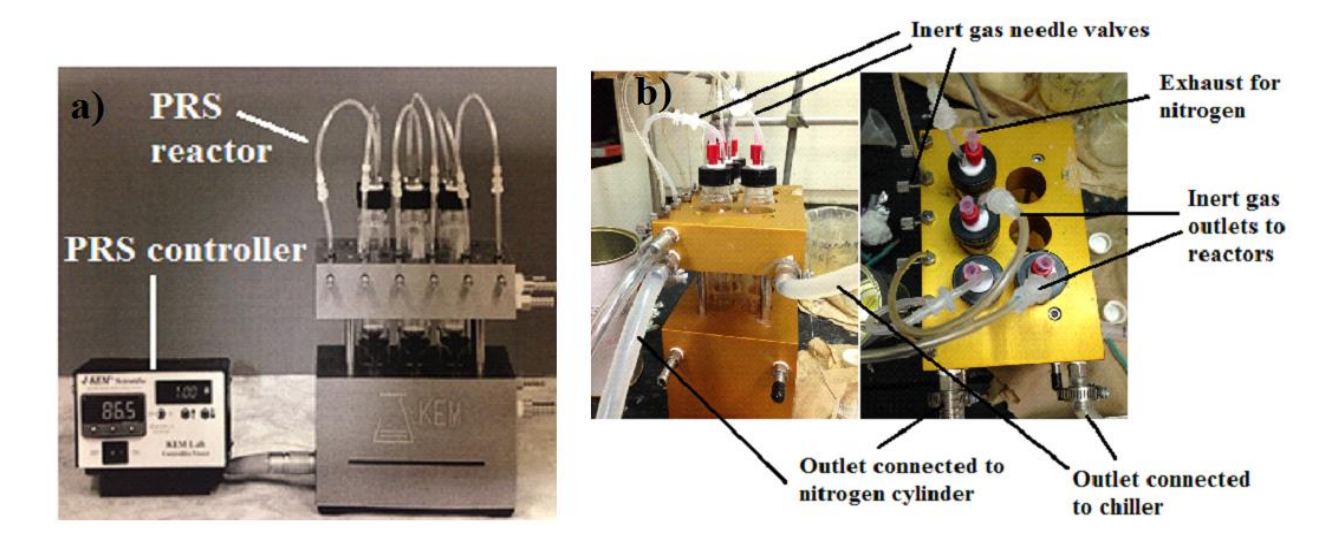


Figure 14. a) General schematic of the PRS set up [27], b) Copolymerization reaction set up.

# 4.2.2. Synthesis of MA/AN/IDBA and MA/AN/AMS with AIBN

A conventional free-radical polymerization, of MA/AN/IDBA, with the initial molar composition,  $f_{MA,0} = 0.50$ ,  $f_{AN,0} = 0.40$ , in 50wt% N, N dimethylformamide (DMF) was conducted at 70 ° C for 3 hours. The polymerization was performed in a 50 mL three-neck round bottom glass flask equipped with a magnetic stir bar, condenser, and thermal well. The flask was set inside a heating mantle and placed on a magnetic stirrer. The central neck was connected to a condenser and capped with a rubber septum with a needle to relieve pressure applied by the nitrogen purge throughout the reaction. A thermocouple was connected to a controller and inserted into the second neck of the flask. The initiator (AIBN, 0.11 g, 0.7 mmol), and the stirrer were added via the third neck of the flask, which was then sealed with a rubber septum. Previously purified MA (6.14 g, 70.6 mmol), AN (3.02 g, 56.5 mmol), IDBA (2.75 g, 14.1 mmol) and DMF (11.56 g, 158.1 mmol) were each injected into the flask via syringe. As stirring began and the monomers were well mixed, the chilling unit using a glycol/water mixture that is connected to the condenser was set to 4 °C. A nitrogen flow was introduced to purge the solution for 30 min. The reactor was then heated to 70

 $^{\circ}$ C while maintaining the purge. The reaction was left for 3 hours, after which the mixture was allowed to cool to room temperature. The final polymer was precipitated in methanol and water, vacuum filtered, and then dried for 120 minutes in a vacuum oven at 50  $^{\circ}$ C. The target number average molecular weight ( $M_{n,target}$ ) at complete conversion, calculated by the mass of monomer relative to the moles of initiator, was set to 17.3 kg/mol. The final yield of the copolymer after 3 hours was 9.2 g (80% conversion of monomers based on  $^{1}$ H NMR analysis) with number-average molecular weight  $M_{n} = 27.7$  kg/mol and polydispersity index  $M_{w}/M_{n} = 3.59$  determined by gel permeation chromatography (GPC) calibrated relative to linear PMMA standards in DMF at 50  $^{\circ}$ C. A few drops of phenyl isocyanate were added to the vial before being introduced into the GPC column, to prevent the amines from attaching to the column. The MA and AN molar composition of the terpolymer using  $^{1}$ H NMR analysis were  $F_{MA} = 0.47$  and  $F_{AN} = 0.39$ . The same procedure was repeated for MA/AN/AMS to make a non-functional terpolymer for comparison with the amine functional IDBA terpolymer.

# **4.2.3.** Thermal Properties

The thermal properties of the polymers was measured using thermogravimetric analysis (TGA) and Differential Scanning Calorimetry (DSC). A TGA Q500 (TA Instruments) was used to measure the decomposition temperature of the polymer to set an upper temperature limit for blending. The analysis was done under oxygen rather than nitrogen to simulate the environment in an extruder. The DSC Q2000 (TA Instruments) was used to measure the melting/softening temperature of polymers to set the lower limit for blending. The measurements were done in an aluminum t-zero pan and were calibrated to an empty aluminum t-zero pan.

## 4.2.4. Reactive Blending of MA/AN/IDBA and MA/AN/AMS terpolymer and PE – MAn

MA/AN/IDBA (0.71 g, 20 wt.%) and PE – MAn (2.83 g, 80 wt.%) were mechanically mixed at room temperature, then fed into a miniature conical counter rotating twin screw extruder (Haake Minilab) at 140 °C. The screw speed was set to 50 rpm. The material was in the extruder for 30 minutes and then quenched immediately (within 15 seconds) in liquid nitrogen to maintain the morphology of the blend. The same procedure was followed for the MA/AN/AMS terpolymer under the same conditions. Electron microscopy was used to determine the microstructure of the blend that in turn could be used to infer whether any reaction occurred.

Samples were also annealed at 130 °C (above the glass transition temperatures of MA/AN/IDBA and PE – MAn as well as the melting point of PE – MAn) for 18 hours to compare against the quenched samples to determine the stability of the microstructure. This was repeated for a 40 wt. %/60 wt. % ratio of MA/AN/IDBA/PE – MAn. The procedure was also repeated using the same extrusion and annealing conditions for the non – functional MA/AN/AMS polymer and PE – MAn blend to analyze the effects of adding an amine group on the microstructure of the polymer.

# 4.2.5. Sample preparation for microscopy

The blend samples were freeze fractured in liquid nitrogen and a portion of the sample was annealed at 130 °C as described in section 4.2.3. The annealed and non-annealed samples were placed in DMF for a period of 6 hours to selectively remove the dispersed terpolymer phase. The samples were then thoroughly air-dried at room temperature and glued onto aluminum stubs. The samples were then sputter-coated with 3 nm of platinum in preparation for scanning electron microscopy (SEM) to make the sample conductive. Then, the microstructure of the blends was viewed with a Hitachi S-4700 Field Emission Scanning Electron Microscope (FE-SEM) at an accelerating voltage of 10 kV.

# 4.2.6. Image Analysis

From the scanned transparency, the areas  $A_i$  of  $n_i$  particles were measured using ImageJ Version 1.45s software. The  $A_i$  were converted to an equivalent sphere diameter  $D_i$ . At least 300 particles were counted from each sample to ensure reliable statistics. The size of the dispersed phase was characterized by the volume to surface average diameter,  $\langle D \rangle$ vs, which gives the average interfacial area per unit volume that can be used to estimate copolymer coverage at the interface [28].  $\langle D \rangle$ vs was calculated by using **Equation 7** found in the literature [29].

$$\langle D \rangle_{vs} = \frac{\sum_{i=1}^{k} n_i D_i^3}{\sum_{i=1}^{k} n_i D_i^2}$$
 (Equation 7)

### 4.2.7. Characterization

# **Gel Permeation Chromatography**

Molecular weights (number average molecular weight  $M_n$ , weight average molecular weight  $M_w$ ) and dispersity  $M_w/M_n$  were estimated using gel permeation chromatography (Waters Breeze) with DMF as the mobile phase at a flow rate of 0.3 mL  $\cdot$  min<sup>-1</sup>. The GPC was equipped with three Styragel® HR columns (HR1 with molecular weight measurement range of 102 to  $5\times102$  g  $\cdot$  mol<sup>-1</sup>, HR2 with molecular weight measurement range of  $5\times102$  to  $2\times104$  g  $\cdot$  mol<sup>-1</sup> and HR4 with molecular weight measurement range of  $5\times103$  to  $6\times105$  g  $\cdot$  mol<sup>-1</sup>) and a guard column. The columns were kept at 50 °C during the analysis and the molecular weights were estimated relative to linear PMMA (Polymethyl methacrylate) standards. The GPC was equipped with both differential refractive index (RI 2410) and ultraviolet (UV 2487) detectors for which the RI detector was used solely for the experiments described herein.

## **Proton Nuclear Magnetic Resonance**

A Varian Mercury-300 NMR (Nuclear Magnetic Resonance) spectrometer was used to determine the molar composition and conversion of the copolymer and terpolymers. MestreNova® software was used to analyze the  ${}^{1}$ H NMR spectra. The copolymers were dissolved in deuterated chloroform (CDCl<sub>3</sub>) and the chemical shifts were reported in parts per million (ppm) using tetramethylsilane (TMS) as a reference The copolymer compositions were calculated using the method published in literature [1] using the formulae listed below where: m = IDBA/AMS content in the copolymer, n = MA content in the copolymer copolymer, n = MA content in the copolymer copolymer.

$$n = \frac{x}{3}$$
 and  $m_{IDBA} = \frac{y}{4}$ ,  $m_{AMS} = \frac{y}{5}$ 

The same method was used to calculate the copolymer compositions of the terpolymers. In this case, the methylene protons for MA and AN overlapped so l = AN content in the copolymer, m = IDBA/AMS content in the copolymer, n = MA content in the copolymer. So then x = the integral, because of the methyl proton from the MA monomer only  $\delta$ : 3.6 (s, 3H, O-CH<sub>3</sub>), y = the integral due to the benzylic protons from IDBA/AMS 6.9 - 7.5 (m, 4H/5H, Ar H) and z = the integral, because of the methylene protons from MA and AN both 1.6 - 2.2 (m, 2H, CH-CH<sub>2</sub>).

$$l_{AN} = \frac{z}{2} - \frac{x}{3}$$
,  $n_{MA} = \frac{x}{3}$  and  $m_{IDBA} = \frac{y}{4}$ ,  $m_{AMS} = \frac{y}{5}$ 

The conversion of the monomers in the reactor was also calculated using <sup>1</sup>H NMR analysis, by tracking the vinyl peaks of each of the monomers. These peaks were distinguished by superimposing the pure monomer spectra(s) onto the polymer spectra. For MA, the vinyl peaks

were δ: 5.8 ppm (1 H, m), 6.2 ppm (1 H, m) and 6.4 ppm (1 H, m). For AN, the vinyl peaks were δ: 5.6 ppm (1 H, m), 6.1 (1 H, m) and 6.2 (1 H, m). For IDBA, the vinyl peaks were δ: 5.1 ppm (1 H, s) and 5.4 ppm (1 H, s). For AMS, the vinyl peaks were 5.0 ppm (1 H, s) and 5.3 ppm (1 H, s). <sup>1</sup>H NMR analysis was done for samples taken every 60 minutes and the peaks on the <sup>1</sup>H NMR spectra were integrated. The decrease in the size of the peaks was noted. For molecules with multiple vinyl peaks, the average integrated area (I<sub>i</sub>) was taken in order to represent the presence of the respective monomer. The individual monomer conversion was calculated using **Equation 8**.

$$X_i = 1 - \left(\frac{l_i}{f_i}\right)$$
 (Equation 8)

 $X_i$ : Conversion of monomer i,  $I_i$ : Average integrated area of monomer i,  $f_i$ : Initial mole feed ratio of monomer i.

The overall conversion of the reaction was calculated using **Equation 9** where X is the overall conversion.

$$\mathbf{X} = \sum \mathbf{X_i} \cdot \mathbf{f_i}$$
 (Equation 9)

### **Thermal Properties**

The thermal properties of the polymers were measured using thermogravimetric analysis (TGA) and differential scanning calorimetry (DSC). A TGA Q500 (TA Instruments) was used to measure the decomposition temperature of the polymer to set an upper temperature limit for blending. The analysis was done under oxygen rather than nitrogen to simulate the environment in an extruder. The DSC Q2000 (TA Instruments) was used to measure the melting/softening temperature of

polymers to set the lower limit for blending. The measurements were done in an aluminum t-zero pan and were calibrated to an empty aluminum t-zero pan.

# **Image Analysis**

The final blended polymer was characterized using a Hitachi S-4700 Field Emission Scanning Electron Microscope (FE-SEM) at an accelerating voltage of 10 kV. The polymer was coated with 3 nm platinum to make it conductive and then images of the surface were taken using SEM.

#### 4.3. Results and Discussion

## 4.3.1. Investigating copolymerization behaviour of MA/IDBA and MA/AMS

Much of our knowledge of the reactivity of monomers and free radicals in chain polymerization comes from copolymerization studies. The behavior of monomers in copolymerization reactions is especially useful for studying the effect of chemical structure on reactivity. Copolymerizations can allow us to tailor and optimize a polymer using different monomer feed ratios and conditions to change the properties of the copolymer. These copolymers fall into different microstructure categories such as *statistical*, *random* or *alternating*. In a random copolymer, the two monomers are distributed randomly throughout the chain [19]. A series of poly(acrylonitrile-co-methyl acrylate) copolymers of differing copolymer compositions were synthesized via free radical polymerization [30], [31]. IDBA has been copolymerized with MMA (methyl methacrylate) by Trumbo *et al.* [17]. According to the data, as more IDBA was fed, the amount of MA incorporated into the polymer increased, as reflected by the final copolymer compositions. For example, experiment 2 in **Table 3** contained  $f_{IDBA, 0} = 0.10$  and  $f_{MA,0} = 0.90$  so the  $F_{MA} = 0.867$ , however, in experiment 3 and 4, when the amount of IDBA was increased to  $f_{IDBA, 0} = 0.20$  and  $f_{IDBA, 0} = 0.30$ , the  $F_{MA}$  values were larger than expected (0.851 at a conversion of 56.2% and 0.723 at a conversion

of 25.3% respectively). This was similar to the results published by Trumbo *et al.* for MMA and IDBA where initial monomer feed compositions,  $f_{\text{MMA},0} = 0.35$  and  $f_{\text{IDBA}, 0} = 0.65$  gave a final polymer composition of  $F_{\text{MMA}} = 0.44$  and  $F_{\text{IDBA}} = 0.56$  at a conversion of 5.7% [17].

Table 3. Copolymerization conditions and results for MA and IDBA

	Monomer in In	nomer in Initial Feed Monomer in Copolymer <sup>2</sup>		Copolymer <sup>2</sup>		
Exp no.1					Time	Conversion <sup>2</sup>
	f <sub>IDBA,0</sub>	f <sub>MA,0</sub>	F <sub>IDBA</sub>	FMA	( <b>h</b> )	(%)
1	0.050	0.950	0.058	0.941	0	15.0
2	0.100	0.900	0.132	0.867	0	7.5
3	0.200	0.800	0.149	0.851	0	56.2
4	0.300	0.700	0.277	0.723	0	25.3

The reactivity ratios of the two monomers were calculated using the linearized form of the Mayo – Lewis equation (**Equation 5**) [23]. The parameters for the equation are shown in **Table 4**. The f(1 - F)/F parameter was plotted against the  $f^2/F$  parameter. The intercept was used to calculate the value of  $r_{MA} = 0.69$  ( $r_2$  in the equation) and the slope was used to calculate the value of  $r_{IDBA} = 1.36$  ( $r_1$  in the equation). The plot is shown in **Figure 15(A)**. Error values were estimated from standard errors in the slope and intercept of the Mayo – Lewis plot. Since the conversions associated with the data in **Table 4** were relatively high for some data points ( $\sim 20-50\%$ ), these results were considered to be affected by compositional drift and may be crude estimates for the actual relative reactivities of the monomers.

<sup>&</sup>lt;sup>1</sup> All reactions were carried out using DMF solvent (at 50 wt % ratio with monomers), a temperature of 70 °C for 2 hours but data is taken for within the first hour of the experiments to ensure low conversion data (and avoid compositional drift)

<sup>&</sup>lt;sup>2</sup> Conversions and mole ratios were determined through <sup>1</sup>H NMR spectroscopy. Conversions were relatively high for Mayo – Lewis calculations, especially for experiment 3 due to temperature overshoot.

Table 4. Linear Mayo – Lewis equation parameters for IDBA and MA copolymerizations

Exp no.	$f = f_{IDBA}/f_{MA}$	F = F <sub>IDBA</sub> /F <sub>MA</sub>	Mayo - Lewis equation parameters		_		IDBA r <sub>IDBA</sub> <sup>3</sup>	MA r <sub>MA</sub> <sup>3</sup>
			f <sup>2</sup> /F	f(1 - F)/F				
1	0.053	0.062	0.045	0.801				
2	0.111	0.152	0.073	0.585	$1.36 \pm 1.60$	$0.69 \pm 0.50$		
3	0.176	0.080	0.390	2.032				
4	0.250	0.175	0.348	1.164				
5	0.429	0.383	0.466	0.681				

The results were also analyzed based on the non – linear or instantaneous form of the Mayo – Lewis equation (**Equation 4**) [23]. This equation was fit to the data points using adjustable parameters and the solver function in Microsoft Excel (2010). The conversions for this data set were high, so very different reactivity ratios compared to the linear Mayo – Lewis analysis were seen, as shown in **Table 5**. However, the trend was the same, with IDBA having a greater reactivity ratio than MA. In both cases however, it seems that IDBA tends to add to itself slightly, which is somewhat surprising since α-methyl styrenics do not readily homopolymerize [17].

<sup>&</sup>lt;sup>3</sup> These are reactivity ratios were calculated using the linear Mayo – Lewis equation plot and are affected by compositional drift so have limited accuracy. The errors were calculated based on standard errors in the slope and y-intercept of the Mayo – Lewis plot.

Table 5. Non – Linear Mayo – Lewis parameters for IDBA and MA

Exp no.	f <sub>IDBA</sub> /f <sub>1</sub>	f <sub>MA</sub> /f <sub>2</sub>	Fidba/F1	F <sub>MA</sub> /F <sub>2</sub>	IDBA r <sub>IDBA</sub> <sup>4</sup>	MA r <sub>MA</sub> <sup>4</sup>
1	0.05	0.95	0.058	0.942		
2	0.1	0.9	0.132	0.868	0.067	0.01
3	0.15	0.85	0.074	0.926		
4	0.1993	0.8007	0.149	0.851		
5	0.29	0.71	0.277	0.723		

Kelen and Tüdos (the K–T method) refined the linear analysis of reactivity ratios by introducing a positive constant  $\alpha$  into the equation, which was used to calculate  $\eta$  and  $\xi$  terms. This allowed the spread of data more evenly and elimination of the bias that was associated with the linearized Mayo – Lewis equation [20]. The values calculated from the plot (shown in **Figure 15C**) were  $r_{MA} = 0.30$  and  $r_{IDBA} = 5.09$ . The reactivity ratios based on this method followed the same trend of  $r_{IDBA} > r_{MA}$ . Error values for this method were difficult to calculate since the solver function was used and the mole ratios were calculated using  $^1H$  NMR analysis.

 $<sup>^4</sup>$  These are reactivity ratios were calculated using the non-linear Mayo – Lewis equation and the Microsoft excel (2010) numerical solver hence they are just estimated values and cannot be used for further calculations.

Table 6. Parameters for the K-T method for MA and IDBA copolymerization

	$\mathbf{F}^5 = \frac{F_{IDBA}}{F_{MA}}$	$\mathbf{f}^6 = \frac{f_{IDBA}}{f_{MA}}$	$\mathbf{H} = \frac{F^2}{f}$	$G = \frac{F(f-1)}{f}$	$\eta^7 = \frac{G}{\alpha + H}$	$\xi = \frac{H}{\alpha + H}$
1	0.062	0.053	0.072	-1.109	-4.813	0.313
2	0.080	0.111	0.220	-1.296	-3.421	0.582
3	0.175	0.250	0.124	-0.534	-1.890	0.439
4	0.383	0.429	0.347	-0.523	-1.035	0.687

Kelen and Tüdos improved their method one step further (extended K–T) to consider the effect of conversion on the polymer and comonomer compositions [32]. This extended K – T equation was used to calculate the reactivity ratios at high conversions. The intercepts at  $\xi=1$  and at  $\xi=0$  of the plot of  $\eta$  against  $\xi$  (shown in **Figure 15B**) gives  $r_1$  ( $r_{IDBA}$ ) and  $r_2/\alpha$  ( $r_{MA}/\alpha$ ), respectively. The values calculated from the graph were  $r_{MA}=0.32$  and  $r_{IDBA}=5.51$ . The errors here were again difficult to calculate since the mole ratios and conversion values were calculated based on  $^1H$  NMR data analysis.

Table 7. Parameters for extended K-T method for MA and IDBA copolymerization

	Conversion (w)	$\mathbf{F}^5 = \frac{F_{IDBA}}{F_{MA}}$	$\mathbf{f}^6 = \frac{f_{IDBA}}{f_{MA}}$		$\xi 1 = \frac{f}{\xi 2 \left(\frac{f}{F}\right)}$	$Z = \frac{\log(1-\xi 1)}{\log(1-\xi 2)}$	$\mathbf{H} = \frac{f}{z^2}$	$G = \frac{(f-1)}{Z}$	$ \eta^8 = \frac{G}{\alpha + H} $	$\xi = \frac{H}{\alpha + H}$
1	0.15	0.062	0.053	0.153	0.130	0.843	0.074	-1.123	-4.846	0.319
2	0.075	0.080	0.111	0.081	0.056	0.682	0.226	-1.313	-3.418	0.589
3	0.562	0.175	0.250	0.507	0.716	1.776	0.078	-0.424	-1.796	0.332
4	0.253	0.383	0.429	0.242	0.267	1.121	0.336	-0.515	-1.042	0.681

<sup>&</sup>lt;sup>5</sup> F<sub>IDBA</sub> is the mole fraction of IDBA in the polymer, F<sub>MA</sub> is the mole fraction of MA in the polymer

 $<sup>^6\,</sup>f_{IDBA}$  is the initial feed ratio of IDBa and  $f_{MA}$  is the initial feed ratio of MA

 $<sup>^{7}</sup>$   $\alpha = \sqrt{H_{\text{max}}H_{\text{min}}} = 0.158$ 

 $<sup>^{8}</sup>$   $\alpha = \sqrt{H_{max}H_{min}} = 0.158$  and  $\mu = molecular$  weight of MA/molecular weight of IDBA = 0.491

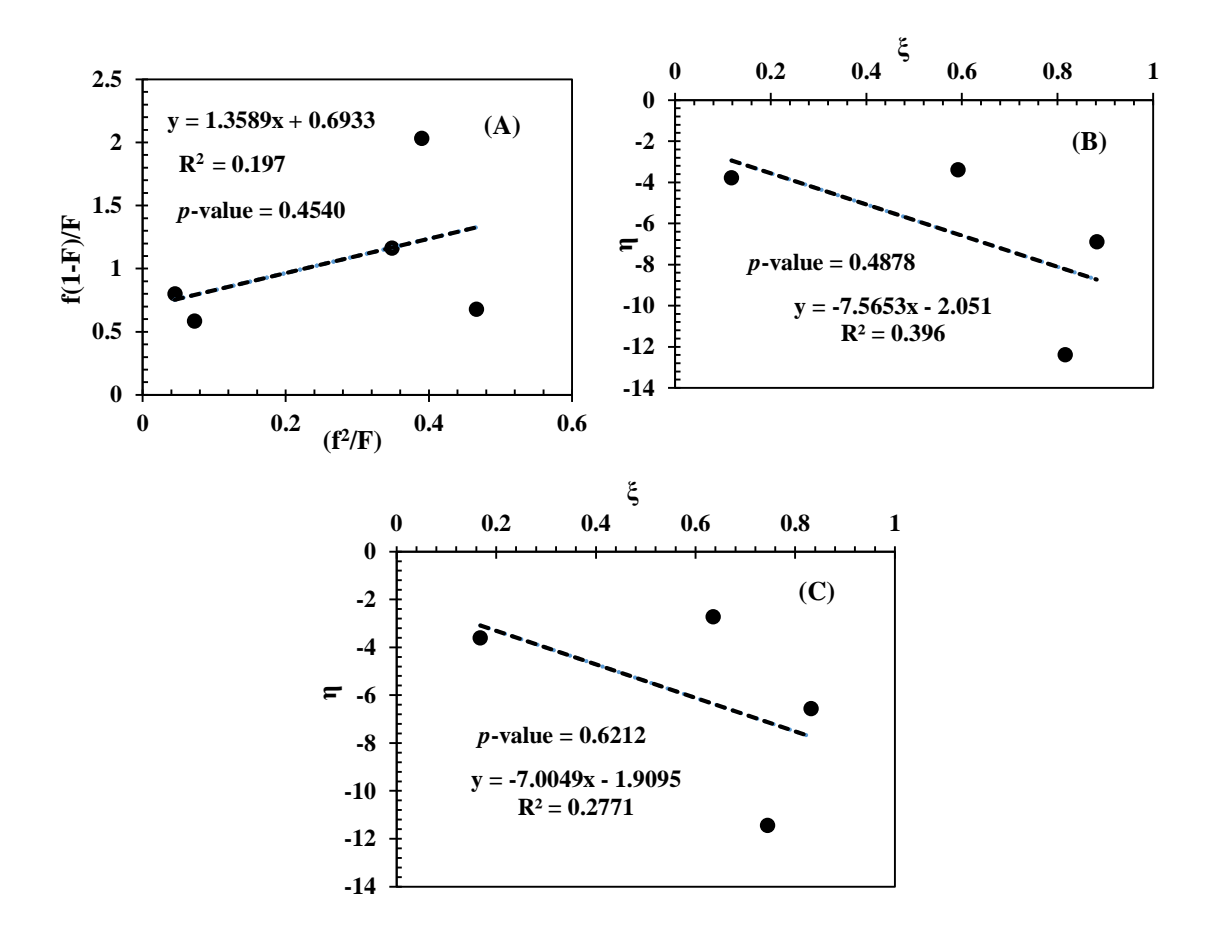


**Figure 15.** (A) Linear Mayo – Lewis plot for MA/IDBA copolymerization, (B) Extended Kelen–Tüdos (extended K–T) plot, (C) Kelen–Tüdos plot (K – T)

For the graphical methods shown in **Figure 15**, the correctness of the polymerization mechanism depends on the linearity of the data points. The  $R^2$  values are so low that predictions are fraught with error and cannot be used to predict copolymer compositions well. The p-values obtained for all the plots in **Figure 15** are high. The p-values help determine significance of the data. The p-value can be a number between 0 and 1. The p-values in this case are >0.05 and a large p-value indicates weak evidence against the null hypothesis, so you fail to reject the null hypothesis. This means that the data is not significant in this case. In addition to obtaining a wider data set, perhaps the implicit assumption about application of the Mayo-Lewis and related equations is not valid.

The Mayo-Lewis equation is a terminal model, in that it assumes that the reactivity is dependent only on the identity of the monomer unit at the growing end and independent of the chain composition preceding the last monomer unit (i.e. terminal model). The extended Kelen-Tüdos method however, does take polymer conversion into account. Using these assumptions the reactivity ratios of IDBA and MA were calculated using data from experiments 1 - 5 in **Table 3**. Copolymerizations can have their microstructure classified or suggested based on the products of their reactivity ratios. For an ideal random copolymerization, the product of  $r_1r_2$  is unity. For  $r_1r_2$ < 1, an alternating copolymerization is expected. For random copolymerization, the product of  $r_1r_2$ approaches unity [19]. **Table 8** shows the values for the r<sub>IDBA</sub>r<sub>MA</sub> product but the values of the reactivity ratios calculated did not agree with literature since IDBA is not likely to homopolymerize however, the analysis in this section suggested otherwise. The data sets were not sufficient for accuracy and conversions were too high. Taking the R<sup>2</sup> values and the p-values into consideration, it was concluded that these calculations would need to be repeated with a larger data set (at conversions <10%) to precisely determine the reactivity ratios of the monomers in this system.

**Table 8.** Summary of reactivity ratios for MA and IDBA copolymerization

	Mayo – Lewis	Mayo – Lewis	Kelen- Tüdos	Kelen– Tüdos
	linear	instantaneous		extended
ridba	1.36	0.067	5.09	5.51
r <sub>MA</sub>	0.69	0.01	0.30	0.32
ridbarma	0.94	0.00067	1.54	1.78

Similarly, MA was copolymerized with AMS at various compositions. The results are summarized in **Table 9**.

Table 9. Copolymerization conditions and results for MA and AMS

	Monomer i	n Feed	Monomer in	Copolymer <sup>10</sup>		
Exp no.9					Time	Conversion <sup>10</sup>
	f <sub>AMS,0</sub>	$f_{MA,0}$	F <sub>AMS</sub>	$F_{MA}$	(h)	(%)
1	0.050	0.950	0.0	1.0	0	11.7
2	0.100	0.900	0.0	1.0	0	19.0
3	0.150	0.850	0.0	1.0	0	-
4	0.200	0.800	0.0	1.0	0	-

A similar range of feed compositions was also used for the copolymerization of AMS with MA (without amine group present) to study the effect of the amine functionality. The results are shown in **Table 9**. Only low conversion data could be analyzed due to the depropagation effects of AMS. AMS has a relatively low ceiling temperature (61 °C for bulk monomer) [45]. Copolymerization of AMS had to take into account depropagation because of its unusually low ceiling temperature. This depropagation effect has been studied in literature for MMA and AMS copolymer [46]. If two vinyl monomers are copolymerized under conditions such that one or both may depropagate, the resultant polymer will have an unusual composition and sequence distribution. We would assume that this could be a possible explanation for the results shown in **Table 9** however, further studies of the system at a broader range of compositions with repeated experimentation is required to confirm this claim. In the beginning, there is little bit of conversion (since time = 0 is taken once

<sup>&</sup>lt;sup>9</sup> All reactions were carried out using DMF solvent, a temperature of 70 °C for 2 hours but data is taken for time=0 to ensure low conversion data (to prevent compositional drift)

<sup>&</sup>lt;sup>10</sup> Conversions and mole ratios were determined through <sup>1</sup>H NMR spectroscopy. Conversion values could not be calculated for experiment 3 and 4 because of very large AMS vinyl peaks leading to negative values and error in calculations

the temperature stabilizes at 70 °C) but once most of the MA converts and AMS becomes dominant in the mixture, the AMS cannot add to the polymer since it cannot homopolymerize [45].

# 4.3.2. Synthesis of MA/AN/IDBA and MA/AN/AMS with AIBN

The amino – functional terpolymer of MA, AN and IDBA was synthesized with various initial feed ratios and conditions to form a polymer with sufficient properties for a barrier material and enough functionality for reactive blending/compatibilization as shown in **Table 12**. The first set of experiments were done for 3 hours but then reaction time was increased to 4 hours because it was found to have similar  $M_w/M_n$  (PDI) but higher conversions for some monomer feed ratios.

Table 12. Experimental conditions for the terpolymerizations of MA/AN/IDBA

	Mon	Monomer in Feed		M	onomer	in					
Exp	(n	(mole ratios)		Copolymer <sup>11</sup> (mole		Conv <sup>13</sup>	$\mathbf{M}_{\mathbf{n}}$	M <sub>w</sub> /M <sub>n</sub>	Time	Temp	
no.			ratios)			(%)	(g/mol) <sup>12</sup>	( <b>PDI</b> ) <sup>14</sup>	(h)	(°C)	
	MA	AN	IDBA	MA	AN	IDBA					
	$\mathbf{f}_1$	$\mathbf{f}_2$	<b>f</b> 3	<b>F</b> <sub>1</sub>	$\mathbf{F}_2$	<b>F</b> 3					
1	0.50	0.40	0.10	0.47	0.39	0.14	80.0	27,700	3.59	3	70
2	0.30	0.60	0.10	0.28	0.59	0.13	72.5	27,000	2.98	4	70
3	0.40	0.50	0.10	0.38	0.50	0.12	83.5	25,900	2.24	4	70
4	0.10	0.80	0.10	0.10	0.78	0.12	81.0	27,400	2.50	4	70

The non – functional terpolymer of MA, AN and AMS was synthesized under the same conditions as the functional polymer using various monomer feed ratios. The results are summarized in **Table 13**.

<sup>&</sup>lt;sup>11</sup>Values were determined using <sup>1</sup>H NMR spectroscopy

<sup>&</sup>lt;sup>12</sup>Values were determined through GPC using linear poly(methyl methacrylate) (PMMA) standards in DMF at 50 °C

Exp no.		omer in 10le ratio		Monomer in  Copolymer <sup>13</sup> (mole  ratios)		Conv <sup>15</sup> (%)	$M_n$ $(g/mol)^{14}$	M <sub>w</sub> /M <sub>n</sub> (PDI) <sup>16</sup>	Time (h)	Temp	
	MA	AN	AMS	MA	AN	AMS					
	$\mathbf{f_1}$	$\mathbf{f}_2$	<b>f</b> <sub>3</sub>	$\mathbf{F_1}$	$\mathbf{F}_2$	<b>F</b> <sub>3</sub>					
1	0.50	0.40	0.10	0.38	0.45	0.17	42.5	3,800	1.73	4	70
2	0.30	0.60	0.10	0.28	0.58	0.14	58.5	24,800	1.72	4	70
3	0.10	0.80	0.10	0.08	0.77	0.15	61.5	17,400	1.64	4	70

Table 13. Experimental conditions for the terpolymerizations of MA/AN/AMS

Figure 17 shows the GPC plot and kinetic data of an MA/AN/IDBA synthesis reaction.

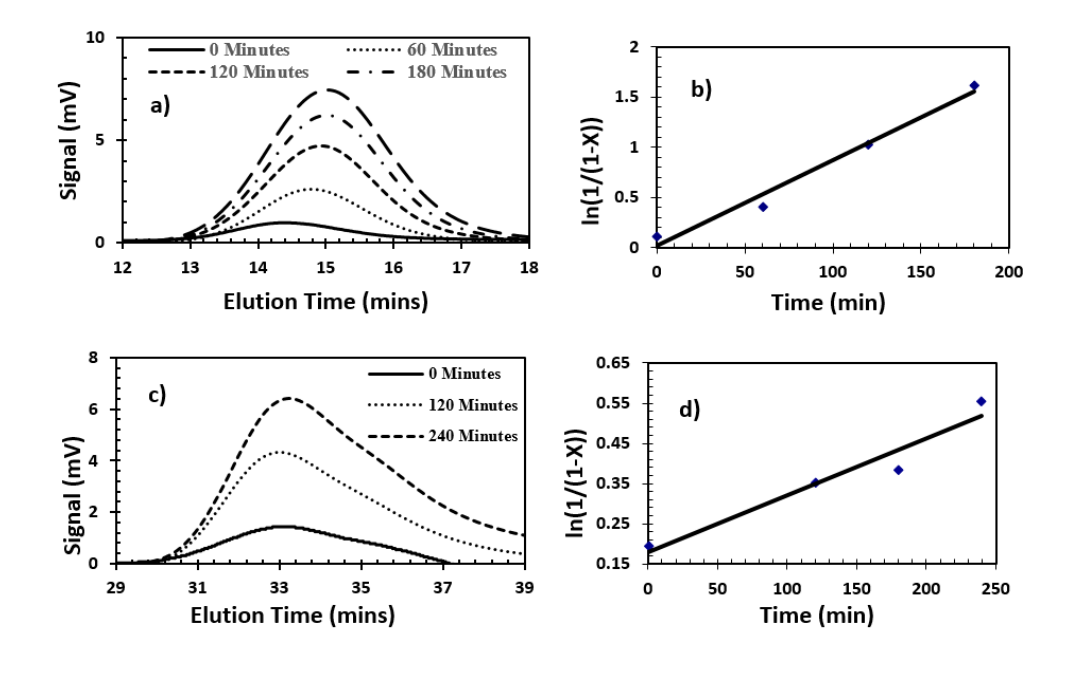


**Figure 17.** (a) GPC plot (DMF, 50 °C) for MA/AN/IDBA terpolymer with initial molar feed compositions  $f_{MA,0} = 0.50$  and  $f_{AN,0} = 0.40$  (b) Plot of  $\ln[(1 - X)^{-1}]$  (X = monomer conversion) versus time for MA/AN/IDBA (c) GPC plot for MA/AN/AMS terpolymer with initial molar feed composition  $f_{MA,0} = 0.50$  and  $f_{AN,0} = 0.40$  (d)Plot of  $\ln[(1 - X)^{-1}]$  (X = monomer conversion) versus time for MA/AN/AMS.

<sup>&</sup>lt;sup>13</sup>Values were determined using <sup>1</sup>H NMR spectroscopy in DMSO-d<sub>6</sub>

<sup>&</sup>lt;sup>14</sup>Values were determined through GPC using linear poly(methyl methacrylate) (PMMA) standards in DMF at 50 °C

According to Figure 17, the kinetic study of the MA/AN/IDBA polymer shows that the molecular weight decreased over time. The results showed that once all the IDBA had converted, the MA and AN polymerized with each other to form smaller chains. This may be due to the fact that the composition changed so much that it caused changes in the hydrodynamic radius. This hypothesis by could be tested analyzing polymer using Matrix-assisted the laser desorption/ionization (MALDI). One of the key advantages of MALDI for synthetic polymer analysis is that the absolute molecular weights of oligomers can be determined as opposed to obtaining relative molecular weights by chromatographic techniques. Since, GPC is a chromatographic technique, the M<sub>n</sub> value calculated is a number average molecular weight and it tabulated an average value for the molecular weight of the long chains along with the small chains. Synthesis of smaller MA/AN chains toward the end of the reaction led to smaller final average values of molecular weight. This was consistently apparent in all monomer feed compositions of MA/AN/IDBA used.

# **4.3.2.** Thermal Stability of Polymers

Since the MA/AN/AMS and MA/AN/IDBA were to be blended in the extruder at a temperature of 140 °C, it was important for them to be thermally stable at this temperature. **Table 14** and **Table 15** summarize the data collected from the TGA and DSC of MA/AN/IDBA and MA/AN/AMS polymers with various compositions.

**Table 14.** Thermal properties of MA/AN/IDBA polymers

Mole	Mole Fraction in Feed (f) <sup>15</sup>		GlassTransition Temperature $T_g$ (°C)	Decomposition Temperature (°C)	$\mathbf{M_n}$ $(\mathbf{g/mol})^{16}$
MA	AN	IDBA	, ,		
50	40	10	-2	160	13,100
30	60	10	-30	140	5,200
40	50	10	-2	130	12,180
10	80	10	16	40	27,400

**Table 15.** Thermal properties of MA/AN/AMS polymers

Mole	Mole Fraction in Feed (f) <sup>17</sup>		GlassTransition Temperature T <sub>g</sub> (°C)	Decomposition Temperature (°C)	$\mathbf{M_n}$ $(\mathbf{g/mol})^{18}$
MA	AN	AMS	, ,		
50	40	10	30	150	3,800
30	60	10	32	140	24,800
10	80	10	35	130	17,400

The decomposition temperature of MA/AN/AMS and MA/AN/IDBA polymers in the  $f_{MA}$  = 0.50,  $f_{AN}$  = 0.40 compositions were 150 °C and 160 °C respectively, so the temperature of extrusion was set at 140 °C for both in order to keep the experimental procedure uniform for the amine functional and non-functional polymers (these compositions were the only ones blended in this study).

# 4.3.3. Reactive Blending of MA/AN/IDBA and MA/AN/AMS with PE – MAn

The amine – functional terpolymer ( $F_{MA}$  = 0.47,  $F_{AN}$  = 0.39,  $F_{IDBA}$  = 0.14) was blended with maleic anhydride grafted poly (ethylene) (PE - MAn) via reactive extrusion. The effectiveness of the amine functionality in the terpolymers in the reactive blends was assessed by comparison of the morphology after melt blending and annealing with the non-reactive analog (PE - MAn with non-functional MA-AN-AMS terpolymer,  $F_{MA}$  = 0.38,  $F_{AN}$  = 0.45,  $F_{AMS}$  = 0.17). The blend morphologies were characterized to determine the level of compatibilization achieved, as witnessed by the dispersed phase particle size (i.e. coalescence was prevented by reactive

 $<sup>^{15}</sup>$ f = mole fraction of monomer in the initial feed for polymerization

<sup>&</sup>lt;sup>16</sup> Values were determined through GPC using linear poly(methyl methacrylate) (PMMA) standards in DMF at 50 °C

compatibilization, which should result in smaller dispersed phase sizes). Further, morphological stability was tested by thermal annealing. The results are summarized in **Table 16**.

MA/AN/IDBA and MA/AN/AMS polymers were separately melt blended with PE – MAn at a 20 wt.% terpolymer loading which is typical for PE barrier blends [33]. It was expected that the primary amine in the MA/AN/IDBA polymer would form imide bonds with the maleic anhydride groups, which are found randomly along the PE - MAn backbone. This would form graft copolymers, which would stabilize the interface between the immiscible PE – MAn and MA/AN/IDBA phases, preventing dispersed phase coalescence and thus a relatively small dispersed MA/AN/IDBA phase domain size would result. The non-functional MA/AN/AMS does not have primary amine groups and thus no copolymer is expected to form at the interface. This non-reactive blend should result in large dispersed phase domains that would coalesce upon annealing [34].

SEM images of the PE – MAn/MA/AN/IDBA and PE – MAn/MA/AN/AMS 80/20 blends are shown in **Figure 18** and images of the 60/40 blends are shown in **Figure 19**. According to the blend morphology characterization shown in **Table 16**, the amine functional blends (MA/AN/IDBA) had smaller particle sizes and upon annealing, the particle size did not change by a considerable amount hence, the blends appeared to be thermally stable. For the non – functional blends (MA/AN/AMS), the particle size found was larger and upon annealing the particle size was seen to increase even further, leading to the conclusion that the blends were less thermally stable compared to the amine – functional blends. This observation helped prove that reactive compatibilization can lead to better blends with PE.

Table 16. Summary of blend microstructure for extruded blends and annealed blends

Terpolymer	Blend Ratio by Wt%	Etching	Annealing	<b>⟨D⟩</b> ν <sub>S</sub> (μm) <sup>17</sup>
sample	(PE-MAn:Terpolymer)	Time (h)	Conditions (°C)	
$F_{MA} = 0.47$	80:20	2	None	0.77±2.2
$F_{AN} = 0.39$ $F_{IDBA} = 0.14$	80:20	6	None	0.78±1.4
	60:40	6	None	1.17±2.6
	80:20	2	68 h at 130 °C	0.60±1.4
$F_{MA} = 0.47$ $F_{AN} = 0.39$ $F_{IDBA} = 0.14$	80:20	6	18 h at 130 °C	0.33±0.7
1 IDBA — 0.14	60:40	6	18 h at 130 °C	1.11±2.5
	80:20	2	None	2.90±6.3
$F_{MA} = 0.38$ $F_{AN} = 0.45$ $F_{AMS} = 0.17$	80:20	6	None	2.59±3.7
1 AMS - 0.17	60:40	6	None	14.9±26.4
$F_{MA} = 0.38$ $F_{AN} = 0.45$	80:20	2	68 h at 130 °C	3.12±6.4
$F_{AMS} = 0.17$	80:20	6	18 h at 130 °C	15.4±29.4
	60:40	6	18 h at 130 °C	25.5±72.5

The  $\langle D \rangle_{VS}$  for the PE – MAn/MA/AN/IDBA blend was consistently smaller than the  $\langle D \rangle_{VS}$  for the PE – MAn/MA/AN/AMS blend as mentioned earlier. This indicated that the PE –

<sup>&</sup>lt;sup>17</sup> Volume to surface area average diameter plus or minus the volume to surface standard deviation

MAn/MA/AN/IDBA blend was able to prevent dynamic coalescence much better compared to the PE – MAn/MA/AN/AMS blend, as was expected. The amine functionalized MA/AN/IDBA successfully reacted with the PE – MAn to form a stabilizing graft copolymer at the interface between the MA/AN/IDBA and PE – MAn. The blends were also annealed to test the thermal stability of the microstructure. Similar trends were found in particle size after annealing where the amine – functional polymer has smaller particle size and seemed to have blended better than the non – functional polymer.

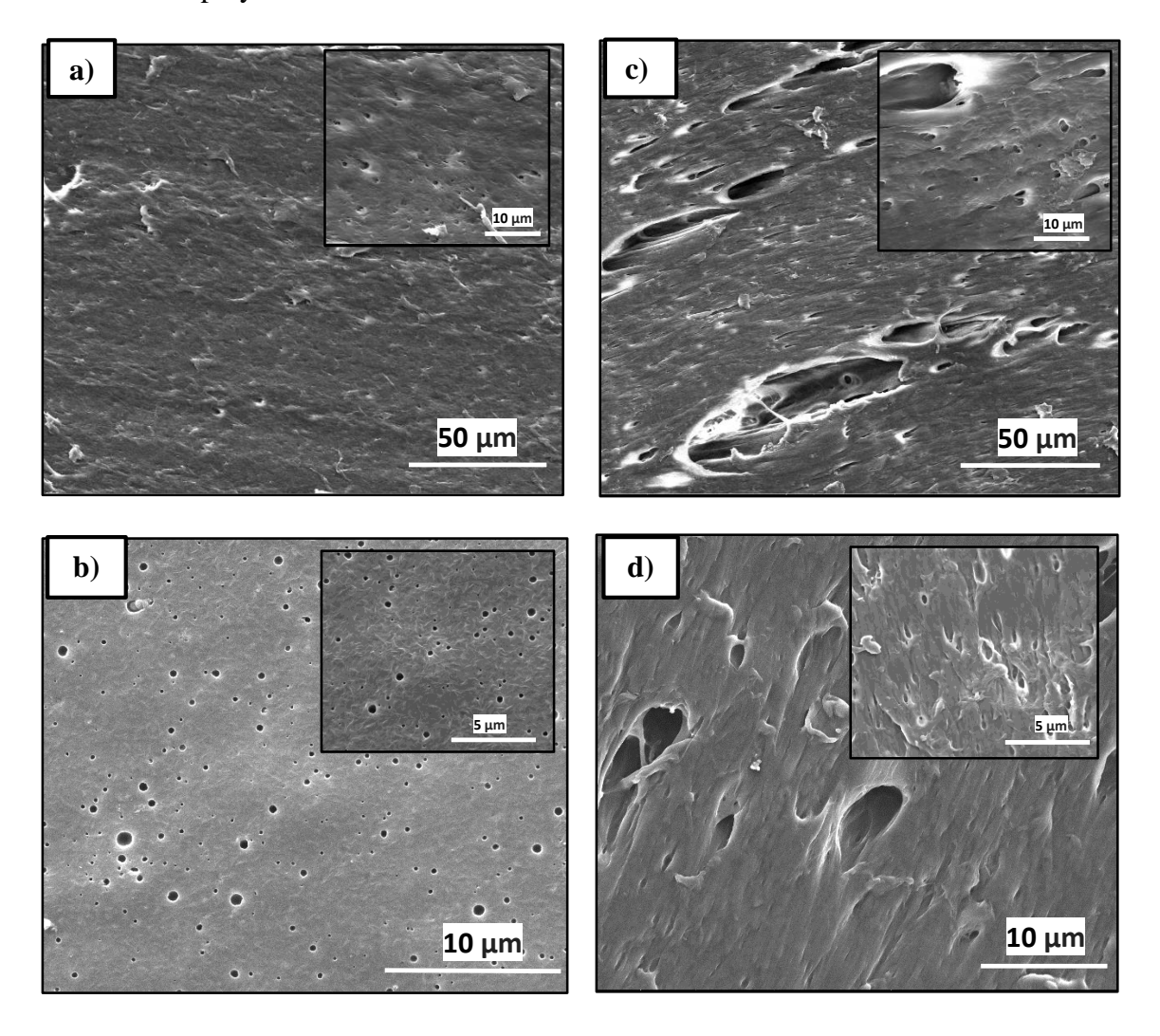


**Figure 18.** SEM images of a) PE-MAn/MA/AN/IDBA (80/20) non-annealed, b) PE-MAn/MA/AN/IDBA (80/20), annealed at 130 °C for 18 hours, c) PE-MAn/MA/AN/AMS (80/20) non-annealed, d) PE-MAn/MA/AN/AMS (80/20), annealed at 130 °C for 18 hours

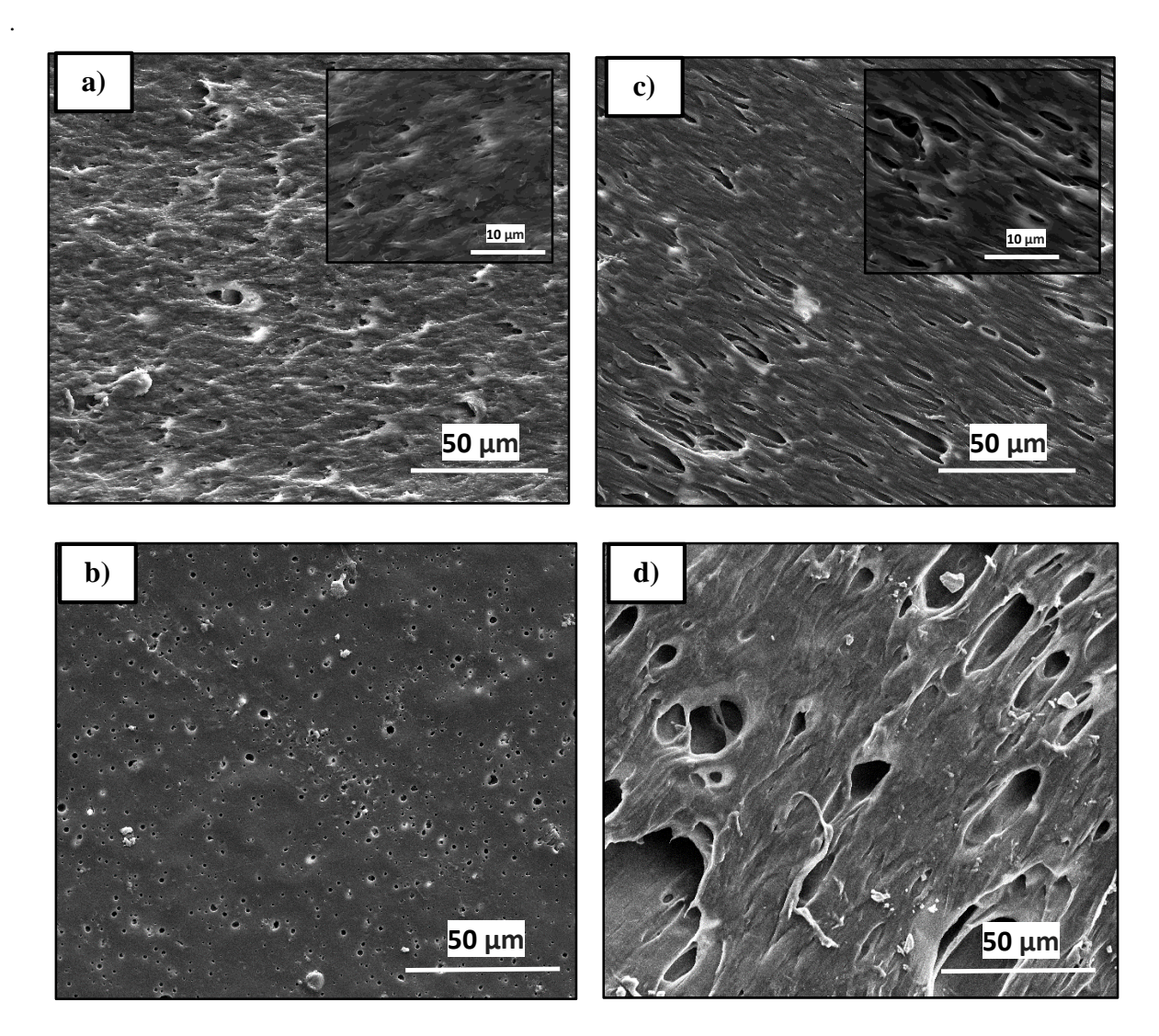


**Figure 19.** a) PE-MAn/MA/AN/IDBA (60/40) non-annealed, b) PE-MAn/MA/AN/IDBA (60/40), annealed at 130 °C for 18 hours, c) PE-MAn/MA/AN/AMS (60/40) non-annealed, d) PE-MAn/MA/AN/AMS (60/40), annealed at 130 °C for 18 hours.

# 4.4. Conclusion

In this chapter, primary amine containing terpolymers were successfully synthesized using conventional free – radical polymerization with AIBN. These functional methyl acrylate/acrylonitrile/IDBA polymers were melt blended with poly(ethylene) grafted with maleic anhydride (PE – MAn). The amine-anhydride reaction was chosen due to its use in commercial

reactive blends such as super-tough nylon and its extremely rapid coupling observed during melt blending [35, 36].

The blend morphology of the dispersed MA/AN/IDBA phase was finer with smaller  $\langle D \rangle_{VS}$  compared to the non-functional MA/AN/IDBA. This showed that the amine-functional polymers were enabling compatibilization of the blend by prevention of dynamic coalescence. This study could broaden the range of applications for barrier materials by producing value-added poly(ethylene) through compatibilization.

### 4.5. Future Work

In order to do an in – depth analysis of the blend morphologies seen in this project, rheological studies should be done to better explain particle size and blending seen in SEM images. These studies can help determine the viscosity ratio of the terpolymer (MA/AN/IDBA or MA/AN/AMS) to the PE – MAn. The viscosity ratio of the two systems influences the dispersion that can be achieved. With a viscosity ratio closer to unity, better dispersion is seen hence, smaller particle sizes. Lower viscosity is associated with larger particle sizes [34]. If these ratios are known, the blend morphology can be further improved by tailoring the properties of the polymers. Furthermore, since the final application of the MA/AN/IDBA/PE – MAn blend was for oil/fuel tanks in this study, future work should focus on testing the oil and gas impermeability and processing properties of these blends. The other MA/AN/IDBA and MA/AN/AMS compositions can also be blended with the PE – MAn to study the effects of different compositions on blending.

#### **CHAPTER 2**

### 1. Introduction

Barrier and membrane polymers are of interest in the oil industry. They need to have several different properties, such as strength, elasticity and durability, in order to fulfill their role. Polyethylene is used as the main material for oil storage, mainly for its cost. However, this material has good water permeability but poor gas permeability [33]. A polyethylene container compatibilized with nylon loses around 1g of hydrocarbon per day [33]. To improve the material's gas permeability, polyethylene is blended with another material. A highly polar polymer is an excellent hydrocarbon barrier but a poor water barrier, while very nonpolar polymers have excellent water barrier properties but poor hydrocarbon barrier properties [37].

Styrene (STY) and acrylonitrile (AN) are found in a copolymer blend called Lopac, which consists of a 70/30 ratio of STY-AN. This polymer is used in food and beverage packaging [37], as the blend consisting of a polar AN and a non-polar STY, it is a good water and hydrocarbon barrier. Lopac was found to have a better oxygen, carbon dioxide, water, ethanol, heptane and ethyl acetate permeability compared to polyethylene [37].

If possible, blending a STY/AN (SAN) copolymer would improve the barrier properties of the polyethylene matrix. However, SAN copolymer is incompatible with polyethylene. Immiscible polymers, when blended together, result in poor dispersions in which the dispersed phase is very large and lacks adhesion to the matrix [33]. This results in unpredictable blend properties [9]. Compatibilizing blends results in more reliable, constant mechanical properties. Compatibilizing can be done through reactive blending, where two compatible functional groups from each phase (or component) of the polymer matrix react together, forming a copolymer during in situ melt

blending, which stabilizes the morphology, reducing the particle size and preventing coalescence of the dispersed phase. How can compatibilization be accomplished? The most common way is to use reactive blending where complementary functional groups on the respective homopolymers can react at the interface during melt blending, forming a copolymer to prevent dispersed phase coalescence and stabilize the morphology. We earlier explored the use of the amine/anhydride coupling, which although effective, requires the synthesis of the amine-containing monomer to be used for reactive blending. It is desirable for an industrial practitioner to use commercially available functional monomers to incorporate into the homopolymer. The focus here is the use of the oxazoline reaction with carboxylic acid [9]. The ideal barrier copolymer must have the functional monomer to promote interfacial adhesion and acrylonitrile to provide the barrier property. Terpolymerizing 2-isopropenyl-2-oxazoline with styrene and acrylonitrile with sufficient acrylonitrile to act as a barrier is one possible route. It can be blended with commercially available 2-isopropenyl-2-oxazoline in order to provide functional monomers for other applications. Finally, these terpolymers can be blended with commercially available polyethylene grafted co-acrylic acid. The structure of the polymer to be synthesized is shown in **Figure 20**.

Figure 20. Structure of statistical STY/AN/iPOx (SAO) polymer

# 2. Research Objectives

SAN copolymers blended with poly(ethylene) were explored as alternative barrier materials in this project. AN was polymerized with 2-isopropenyl-2-oxazoline (iPOx) and styrene (Sty). Oxazoline functionality was required to provide a functional group for reactive compatibilization with the complementary functionalized poly(ethylene). Oxazoline rings can react with carboxylic acids in polymer blends [9]. Acrylonitrile is needed to impart barrier properties – in the past it has been used as a gas barrier material but here we suggest it may be useful as a hydrocarbon barrier. Styrene is added to improve processing as poly(acrylonitrile) is very brittle and degrades easily with excessive heating. Reactive compatibilization is essential for stabilizing the blend morphology and thus control of barrier and mechanical properties. We thus used a statistical 2-isopropenyl-2-oxazoline/acrylonitrile/styrene terpolymer as the dispersed phase to be melt blended with (meth)acrylic grafted polyethylene.

# A) SAO polymerization with AIBN:

Before controlled polymerization could be carried out, the polymerization behaviour of 2-isopropenyl-2-oxazoline (iPOx) with styrene(STY) and acrylonitrile (AN) was tested and the reaction kinetics were observed using conventional polymerization and AIBN initiator. Various compositions of the monomers were used.

# B) Nitroxide Mediated Polymerization (NMP) with NHS - BlocBuilder:

The target styrene (STY), acrylonitrile (AN) and 2-isopropenyl-2-oxazoline (iPOx) terpolymer was synthesized using the controlled radical polymerization technique (CRP) called nitroxide mediated polymerization (NMP). The oxazoline functional co-monomer was used at < 20 mol% in the feed composition since it was only needed to impart compatibilization and does not add to

the barrier material properties. As we are targeting SAN copolymers for barrier applications, the acrylonitrile loading must be sufficiently high for barrier materials but not so excessive as to hinder the processability. Thus, the target acrylonitrile composition was 50-80 mol%.

# C) Blending with Poly(ethylene):

The oxazoline functional terpolymers were synthesized using a succinimidyl ester (NHS) terminated unimolecular initiator based on the nitroxide derived from *N-tert*-butyl-*N*-[1-diethylphosphono-(2,2-dimethylpropyl) nitroxide] (SG1). The terpolymer was blended with polyethylene grafted co-acrylic acid (PE – AA) using solvent casting. The morphologies of these blends were characterized to determine the level of compatibilization achieved with the poly(ethylene) and thermal stability of the microstructure was also tested.

# 3. Compatibilization of STY/AN/iPOx (SAO) with PE - AA

#### 3.1. Materials

Acrylonitrile (AN, ≥99%, contains 35-45 ppm monomethyl ether hydroquinone as inhibitor) and Styrene (STY, ≥99.5%, containing 0.005% 4-tert-butylcatechol as stabilizer) were purchased from Sigma-Aldrich and purified by passing through a column of basic alumina (Brockmann, Type 1, 150 mesh) mixed with 5% calcium hydride (90−95%, reagent grade), then sealed with a head of nitrogen and stored in a refrigerator until needed. *N*, *N*-dimethylformamide (DMF, 99.8%) and tetrahydrofuran (THF, 99.9%) were purchased from Fisher and used as received. 2, 2-Azobis(2 methylpropionitrile) (AIBN, 99%) was purchased from Sigma–Aldrich and used as received. Chloroform-d (CDCl3, 99.8 atom %) was purchased from Cambridge Isotope Laboratories and used as received. Dimethyl sulfoxide-d6 (DMSO-d6, 99.9 atom %) was purchased from Sigma – Aldrich and used as received. *N*-hydroxysuccinimide (98%) and *N*, *N*′-dicyclohexylcarbodiimide (DCC, 99%) were received from Sigma-Aldrich and used in conjunction with BlocBuilder® to

synthesize the N-succinimidyl ester terminated alkoxyamine BlocBuilder (NHS-BlocBuilder) using the same procedure as Vinas et al [38]. Poly(ethylene-*co*-acrylic acid), acrylic acid 5 wt. %, beads (PE – AA) purchased from Sigma – Aldrich and used as received.

## 3.2. Experimental

# 3.2.1. Synthesis of STY/AN/ iPOx (SAO) with AIBN

A traditional (uncontrolled) free-radical polymerization, of STY/AN/ iPOx, with the initial molar composition, f<sub>STY.0</sub> = 0.40, f<sub>AN.0</sub> = 0.50, in 50wt% N, N dimethylformamide (DMF) was conducted at 70 ° C for 5 hours. The polymerization was performed in a 50 mL three-neck round bottom glass flask equipped with a magnetic stir bar, condenser, and thermal well. The flask was set inside a heating mantle and placed on a magnetic stirrer. The central neck was connected to a condenser and capped with a rubber septum with a needle to relieve pressure applied by the nitrogen purge throughout the reaction. A thermocouple was connected to a controller and inserted into the second neck of the flask. The initiator (AIBN, 0.11 g, 0.7 mmol), and the stirrer were added via the third neck of the flask, which was then sealed with a rubber septum. Previously purified STY (1.58 g, 15.2 mmol), AN (1.01 g, 18.9 mmol), iPOx (0.42 g, 3.8 mmol) and DMF (3.0 g, 41.1 mmol) were each injected into the flask via syringe. As stirring began and the monomers were well mixed, the chilling unit using a glycol/water mixture that is connected to the condenser was set to 4 °C. A nitrogen flow was introduced to purge the solution for 30 min. The reactor was then heated to 70 °C while maintaining the purge. The reaction was left for 5 hours, after which the mixture was allowed to cool to room temperature. The final polymer was precipitated in a mixture of methanol and water, vacuum filtered, and then dried for 120 minutes in a vacuum oven at 50 °C. The target number average molecular weight (M<sub>n,target</sub>) at complete conversion, calculated by the mass of monomer relative to the moles of initiator, was set to 4.4 kg/mol. The final polymer has a numberaverage molecular weight  $M_n = 3.5$  kg/mol and polydispersity index  $M_w/M_n = 2.87$  determined by gel permeation chromatography (GPC) calibrated relative to linear PMMA standards in THF at 40 °C. The composition of the terpolymer using <sup>1</sup>H NMR analysis were  $F_{STY} = 0.39$  and  $F_{AN} = 0.51$ . This procedure was repeated using different initial compositions and conditions.

# 3.2.2. Nitroxide Mediated Polymerization of STY/AN/iPOx (SAO) with NHS - BlocBuilder

A nitroxide mediated copolymerization of STY/AN/iPOx in 50wt% N, N-dimethylformamide (DMF) was conducted at 90 °C, using NHS-BlocBuilder. Initial molar composition, f<sub>STY,0</sub> = 0.40,  $f_{AN,0} = 0.50$ , in 50wt% N, N dimethylformamide (DMF) was conducted for 3 hours. The polymerization was performed in a 50 mL three-neck round bottom glass flask equipped with a magnetic stir bar, condenser, and thermal well. The flask was set inside a heating mantle and placed on a magnetic stirrer. The central neck was connected to a condenser and capped with a rubber septum with a needle to relieve pressure applied by the nitrogen purge throughout the reaction. A thermocouple was connected to a controller and inserted into the second neck of the flask. NHS – BlocBuilder is used as the initiator. It is formed from BlocBuilder© to cap the carboxylic acid group in order to prevent the acid group from reacting with the oxazoline ring in the iPOx monomer. The reaction is shown in **Figure 21**. The initiator (NHS - BlocBuilder, 0.168 g, 0.34 mmol), and the stirrer were added via the third neck of the flask, which was then sealed with a rubber septum. Previously purified STY (4.49 g, 43.11 mmol), AN (2.87 g, 54.2 mmol), iPOx (1.20 g, 10.8 mmol) and DMF (8.57 g, 117.3 mmol) were each injected into the flask via syringe. As stirring began and the monomers were well mixed, the chilling unit using a glycol/water mixture that is connected to the condenser was set to 4 °C. A nitrogen flow was introduced to purge the solution for 30 min. The reactor was then heated to 90 °C while maintaining the purge. The reaction was left for 3 hours, after which the mixture was allowed to cool to room temperature.

The final polymer was precipitated in methanol and water, vacuum filtered, and then dried for 120 minutes in a vacuum oven at 50 °C. The target number average molecular weight ( $M_{n,target}$ ) at complete conversion, calculated by the mass of monomer relative to the moles of initiator, was set to 25.0 kg/mol. The final polymer has a number-average molecular weight  $M_n = 9.3$  kg/mol and polydispersity index  $M_w/M_n = 1.32$  determined by gel permeation chromatography (GPC) calibrated relative to linear PMMA standards in THF at 40 °C. The molar composition of the terpolymer using <sup>1</sup>H NMR analysis was  $F_{STY} = 0.13$  and  $F_{AN} = 0.83$ . This procedure was repeated using different compositions and conditions.

**Figure 21.** Dissociation of BlocBuilder, (b) Synthesis of succinimidyl ester terminated BlocBuilder (NHS – BlocBuilder) [39]

### 3.2.3. Chain extension of SAO polymer

Chain extension is performed by adding an amount of STY (8.70 g, 83.5 mmol) and AN (1.77 g, 33.4 mmol) proportional to the amount of styrene/acrylonitrile monomer feed in the original terpolymer ( $F_{STY}$  and  $F_{AN}$ ) to the macro initiator. The macro initiator was the purified SAO-SG1 (From NMP polymerization in section 3.2.2., 1.05 g) and was dissolved in 50wt% N, N

dimethylformamide (DMF), (11.5 g, 157.3 mmol) to the reaction mixture. A 10:1 monomer/macro initiator mass ratio was used for chain extension. A nitrogen flow was introduced to purge the solution for 30 min. The reactor was then heated to 90 °C while maintaining the purge. The reaction was left for 6 hours, after which the mixture was allowed to cool to room temperature. The final polymer was precipitated in a mixture of methanol and water, vacuum filtered, and then dried for 120 minutes in a vacuum oven at 50 °C. The overall conversion was 42.5% and was calculated using <sup>1</sup>H NMR analysis. Gel permeation chromatography (GPC) calibrated relative to linear PMMA standards in THF at 40 °C was used to monitor the increase in molecular weight with the progress of the reaction.

## 3.2.4. Removal of SG1 end group

The SAO polymer had the SG1 group attached to it as shown in **Figure 22**. Permanent removal of the *N-tert*-butyl-*N*-[1-diethylphosphono-(2,2-dimethylpropyl) nitroxide] (SG1) radical was performed as done previously in literature [40]. With the same set-up as described in the previous section, NHS-SAO copolymer and 50 wt% *N*, *N* dimethylformamide (DMF) were added to the 50 mL round bottom flask, and it was sealed as before. A nitrogen flow was introduced to purge the solution for 30 min. AN excess of thiophenol (~ 13 equivalent) was injected into the reaction mixture via syringe. The reactor was heated to 90 °C while maintaining the purge. The reaction was left stirring at 90 °C for 270 min. The solution was allowed to cool to room temperature, and the polymer was precipitated in methanol and water mixture, vacuum filtered, and dried overnight in a vacuum oven at 50 °C. As SG1 has phosphorous in its structure, the removal of the SG1 end-group was confirmed using <sup>31</sup>P NMR spectroscopy.

Figure 22. Structure of Sty/AN/iPOx (SAO) – SG1 terpolymer

## 3.2.5. Thermal Properties of SAO

The thermal properties of the polymers was measured using thermogravimetric analysis (TGA) and Differential Scanning Calorimetry (DSC). A TGA Q500 (TA Instruments) was used to measure the decomposition temperature of the polymer to set an upper temperature limit for blending. The analysis was done under oxygen rather than nitrogen to simulate the environment in an extruder. The DSC Q2000 (TA Instruments) was used to measure the melting/softening temperature of polymers to set the lower limit for blending. The measurements were done in an aluminum t-zero pan and were calibrated to an empty aluminum t-zero pan.

### 3.2.6. Solvent casting of SAO and Acrylic acid Grafted Poly(ethylene)

SAO ( $f_{STY,0} = 50$ ,  $f_{AN,0} = 20$ ,  $f_{iPOx,0} = 30$ ) (0.801 g, 20 wt.%) and PE – AA (3.23 g, 80 wt.%) were mixed together in equal amount of toluene by weight (4.03 g, 43.7 mmol). The PE – AA could not be extruded at temperatures greater than 100 °C whereas SAO required a temperature of 112 °C for blending so solvent casting was used instead of extrusion. The blending was performed in a 25 mL three-neck round bottom glass flask equipped with a magnetic stir bar, condenser, and thermal well. The flask was set inside a heating mantle and placed on a magnetic stirrer. The central neck was connected to a condenser and the other neck was capped with a rubber septum. A thermocouple was connected to a controller and inserted into the third neck of the flask. The temperature was set to 112 °C. The PE-AA dissolved in the toluene and now the SAO and PE –

AA were both dissolved in a common medium allowing them to react. The blending was allowed to continue for 2 hours, after which a precipitate formed in the reactor. The precipitate was allowed to dry in the fume hood at room temperature for 24 hours.

## 3.2.7. Sample preparation for microscopy

The samples were annealed at 120 °C (above the T<sub>g</sub> of SAO and PE – AA as well as the melting point) for 18 hours. The annealed sample was washed and placed in DMF for a period of 2 hours to selectively remove the dispersed terpolymer phase. After this, the sample was thoroughly air-dried at room temperature and glued onto aluminum stubs. It was then sputter-coated with 3 nm of platinum in preparation for scanning electron microscopy (SEM) to make the sample conductive. Then, the microstructure of the blends was viewed with a Hitachi S-4700 Field Emission Scanning Electron Microscope (FE-SEM) at an accelerating voltage of 10 kV.

# 3.2.8. Image Analysis

The exact same procedure as Section 4.2.6. from Chapter 1 was followed, using the same software for analysis.

### 3.2.9. Characterization

<sup>1</sup>H NMR, GPC and FTIR were used for characterization of the polymer and TGA and DSC were used to characterize before blending in the same manner as Section 4.2.7. from Chapter 1.

## 3.3. Results and Discussion

### 3.3.1. Synthesis of SAO with AIBN

Various monomer feed ratios and conditions were used for STY/AN/iPOx to study the properties of the polymer by conventional uncontrolled polymerization (initiator AIBN). The results are summarized in **Table 17**.

Table 17. Characterization of STY/AN/iPOx conventional free radical terpolymers

	Monomer in Feed		Monomer in								
Exp	(mole ratios)			Copolymer <sup>18</sup> (mole			Conv <sup>19</sup>	$\mathbf{M}_{\mathbf{n}}$	M <sub>w</sub> /M <sub>n</sub>	Time	Temp
no.				ratios)			(%)	(g/mol) <sup>19</sup>	(PDI) <sup>20</sup>	(h)	(°C)
	STY	AN	iPOx	STY	AN	iPOx					
	$\mathbf{f_1}$	$\mathbf{f}_2$	$\mathbf{f}_3$	$\mathbf{F_1}$	$\mathbf{F}_2$	<b>F</b> <sub>3</sub>					
1	0.20	0.70	0.10	0.23	0.67	0.10	90.6	19,000	1.95	2	70
2	0.40	0.50	0.10	0.39	0.51	0.09	96.9	9,500	3.19	5	70
3	0.40	0.50	0.10	0.28	0.66	0.06	71.2	4,400	2.96	4	70
4	0.60	0.30	0.10	0.49	0.41	0.10	82.6	6,900	1.80	5	70

# 3.3.2. Nitroxide Mediated Polymerization of STY/AN/iPOx (SAO)

Different monomer feeds for STY, AN and iPOx were used. The temperature and time were changed to optimize the properties of the polymer and attempt to control the dispersity index (PDI or  $M_w/M_n$ ). **Table 18** summarizes the results of the experiments carried out. The relatively low  $M_w/M_n$  (PDI) of the experiments compared to the experiments carried out using AIBN as an initiator provides some indication that a controlled polymerization may be occurring.

<sup>&</sup>lt;sup>18</sup>Copolymer composition was determined using <sup>1</sup>H NMR spectroscopy in CDCl<sub>3</sub>

<sup>&</sup>lt;sup>19</sup>Molecular weights and molecular weight distributions were determined through GPC using linear poly(methyl methacrylate) (PMMA) standards in THF at 40 °C

Table 18. Characterization of STY/AN/iPOx terpolymers made by nitroxide mediated polymerization

	Mon	onomer in Feed Monomer in									
Exp	(mole ratios)			Copolymer <sup>20</sup> (mole			Conv <sup>21</sup>	$\mathbf{M_n}$	M <sub>w</sub> /M <sub>n</sub>	Time	Temp
no.				ratios)			(%)	(g/mol) <sup>21</sup>	( <b>PDI</b> ) <sup>22</sup>	(h)	(°C)
	STY	AN	iPOx	STY	AN	iPOx					
	$\mathbf{f}_1$	$\mathbf{f}_2$	f <sub>3</sub>	$\mathbf{F}_{1}$	$\mathbf{F}_2$	<b>F</b> <sub>3</sub>					
1	0.40	0.50	0.10	0.13	0.83	0.03	59.0	9,300	1.32	3	90
2	0.50	0.30	0.20	0.18	0.75	0.07	39.5	3,500	1.43	4	90
3	0.50	0.20	0.30	0.45	0.27	0.28	74.5	19,500	2.27	5	110
4	0.50	0.20	0.30	0.43	0.31	0.26	65.0	26,400	1.55	24	90

Kinetic studies were also done on the SAO terpolymers synthesized in experiments 1-4 (in **Table 18**). The results from these studies provided some indication that a controlled polymerization was occurring based on the low PDI values. The GPC data for  $M_n$  versus conversion is plotted in **Figure 23**. It shows that the  $M_n$  versus conversion plots were linear (except **Figure 23b** where  $R^2$  value is very small) up to 60-70% conversion and the polydispersities remained low (<1.5 for most) indicating that these polymerizations were substantially living. However, as shown in **Figure 23a** and **d**, the linear trend for  $M_n$  is biased by the high conversion samples - that forces the intercept to go through  $M_n = 0$  at about 20% conversion. The fit is misleading in due to possible branching at high conversion. The data does show that overall, NMP could be used to control the copolymerization of styrene/acrylonitrile copolymers with a low fraction of iPOx (< 30 mol%) at lower conversions (at 74.5 % conversion from **Table 18**, the PDI was much higher and equal to 2.27). The polymerization of iPOx has previously been done in a controlled manner using RAFT

<sup>&</sup>lt;sup>20</sup>Copolymer compositions were determined using <sup>1</sup>H NMR spectroscopy in CDCl<sub>3</sub>

<sup>&</sup>lt;sup>21</sup>Average molecular weights and molecular weight distributions were determined using GPC using linear poly(methyl methacrylate) (PMMA) standards in THF at 40 °C

[41] however, in this polymerization, the reaction slowed down at 30% conversion. Using NMP, the reaction was able to proceed to higher conversions (<65% with low PDI values) than RAFT but it does eventually slow down as was initially observed in literature.

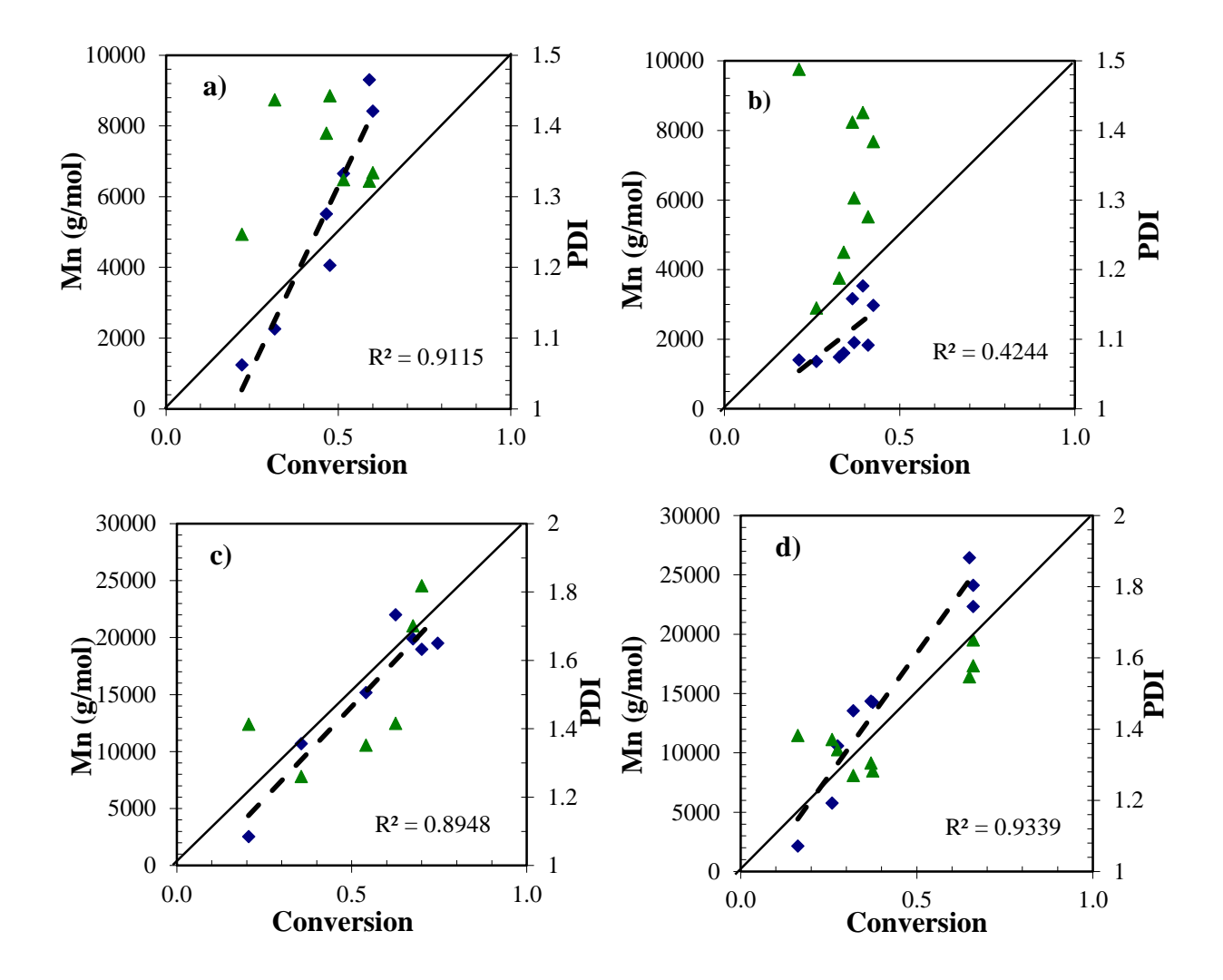


**Figure 23.**  $M_n$  and PDI vs conversion plot of the NMP polymerization of STY, AN and iPOx. Green triangles: PDI, Blue squares: GPC  $M_n$  values. In a)  $f_{STY} = 0.40$ ,  $f_{AN} = 0.50$ ,  $f_{iPOx} = 0.10$  monomer feed ratio, b)  $f_{STY} = 0.50$ ,  $f_{AN} = 0.30$ ,  $f_{iPOx} = 0.20$  monomer feed ratio c)  $f_{STY} = 0.50$ ,  $f_{AN} = 0.20$ ,  $f_{iPOx} = 0.30$  monomer feed ratio (3 hr reaction) d)  $f_{STY} = 0.50$ ,  $f_{AN} = 0.20$ ,  $f_{iPOx} = 0.30$  monomer feed ratio (24 hr reaction)

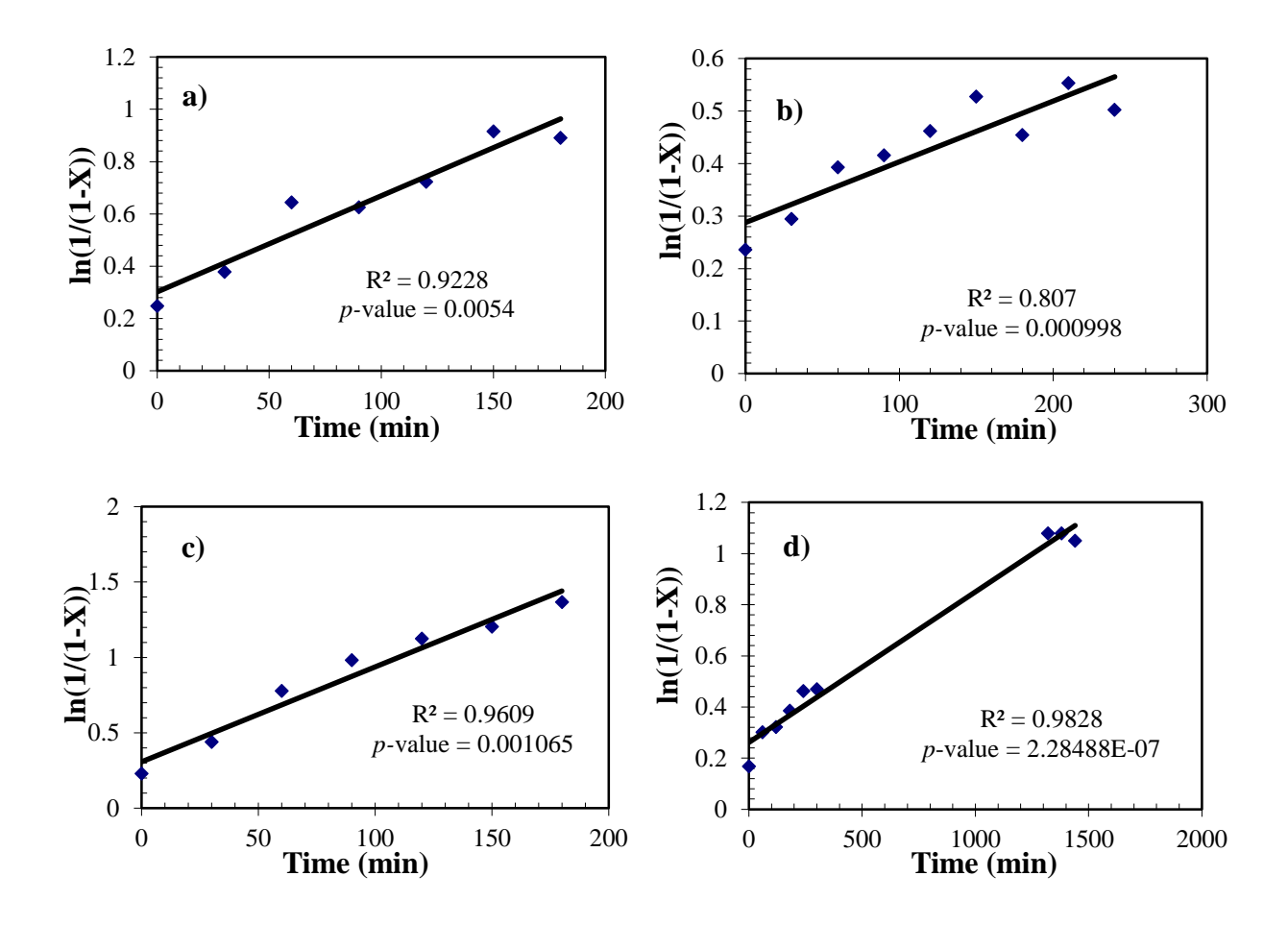


**Figure 24.** Plot of  $\ln[(1 - X) - 1]$  (X = monomer conversion) versus time a)  $f_{STY} = 0.40$ ,  $f_{AN} = 0.50$ ,  $f_{iPOx} = 0.10$  monomer feed ratio, b)  $f_{STY} = 0.50$ ,  $f_{AN} = 0.30$ ,  $f_{iPOx} = 0.20$  monomer feed ratio c)  $f_{STY} = 0.50$ ,  $f_{AN} = 0.20$ ,  $f_{iPOx} = 0.30$  monomer feed ratio (3 hr reaction) d)  $f_{STY} = 0.50$ ,  $f_{AN} = 0.20$ ,  $f_{iPOx} = 0.30$  monomer feed ratio (24 hr reaction)

Figure 24 indicates the scaled conversion for experiments with different monomer feed ratios. These plots show some conversion at t = 0 because this point was taken once the temperature of the reaction had stabilized. It should be noted that the reaction temperatures were above the dissociation temperature of NHS – BB. Hence, the reaction had already started before t = 0. The conversion of the monomers with time increases linearly for reactions done for a shorter duration (shown in **Figure 24c**), whereas reactions done for longer durations (shown in **Figure 24d**) seemed to plateau toward the end of the reaction. As a whole, the reactions appeared to be showing a linear

trend and this supported the claim that NMP can be used to polymerize oxazoline functional polymers in a controlled manner. The  $R^2$  values were used as evidence for the linearity of the trends and the small p-values (<0.05) showed that the results were significant. Further proof of NMP was demonstrated by plotting the elution times of the chains using GPC (**Figure 25**) to show that the chains were growing. There is a clear shift towards higher molecular weights as the reaction proceeded.

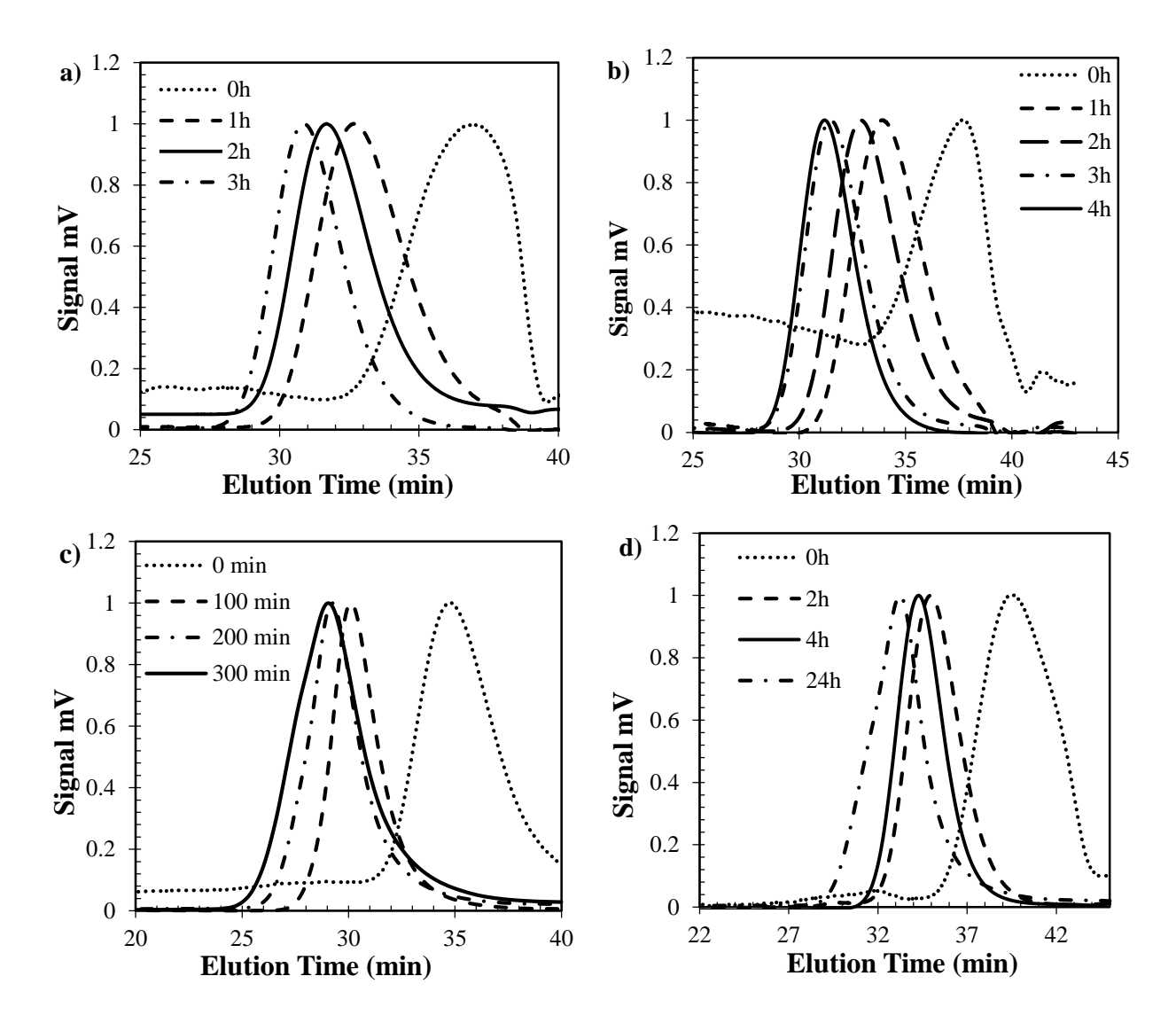


**Figure 25.** GPC plot (THF, 40 °C), using PMMA standards, for SAO terpolymers with initial molar feed compositions a)  $f_{STY,0} = 0.40$ ,  $f_{AN,0} = 0.50$ ,  $f_{iPOx} = 0.10$ , b)  $f_{STY,0} = 0.50$ ,  $f_{AN,0} = 0.30$ ,  $f_{iPOx} = 0.20$ , c)  $f_{STY,0} = 0.50$ ,  $f_{AN,0} = 0.20$ ,  $f_{iPOx} = 0.30$  (3hr reaction), d)  $f_{STY,0} = 0.50$ ,  $f_{AN,0} = 0.20$ ,  $f_{iPOx} = 0.30$  (24 hr reaction)

# 3.3.3. Chain extension of STY/AN/iPOx polymer

Nitroxide mediated polymerization is a form of controlled polymerization. These polymers retain their ability to propagate and grow whenever monomers are supplied [42]. In order to show that the SAO polymers synthesized using NMP have sufficiently active SG1-terminated chain ends, a series of chain extensions were carried out with styrene/acrylonitrile monomer mixtures. Kinetic studies were done to monitor the progress of the reaction and the growth of the polymer chains was analyzed using GPC plots of elution time as shown in **Figure 26**.

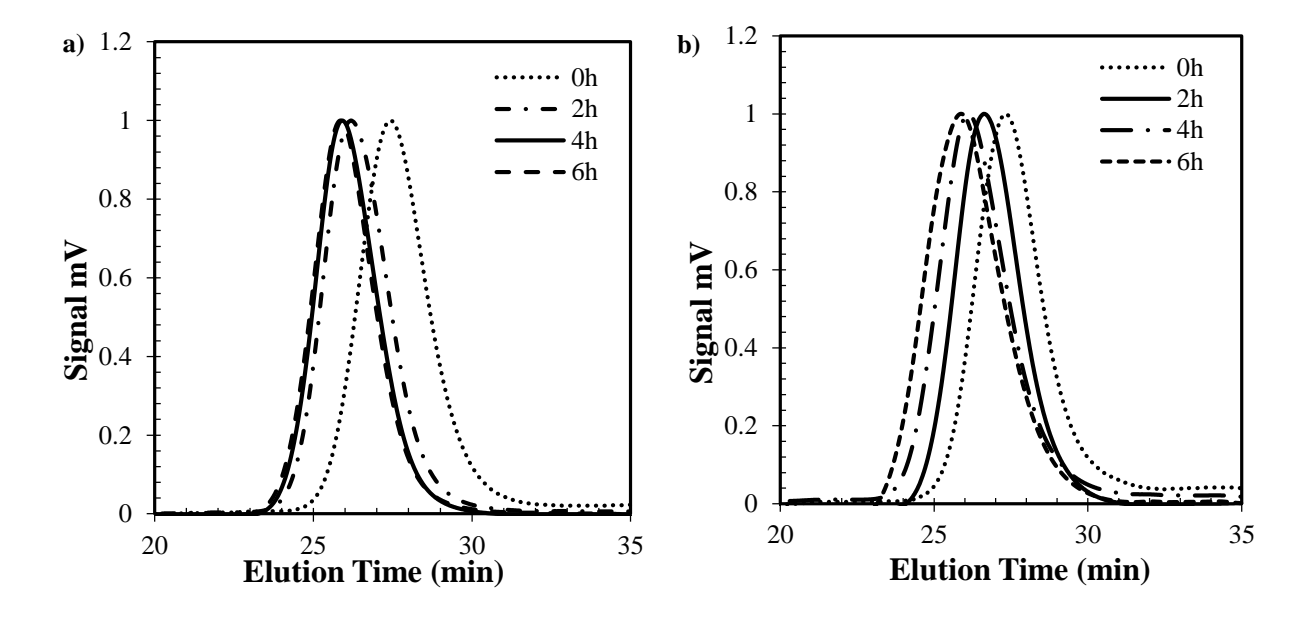


**Figure 26.** GPC plot (THF, 40 °C), using PMMA standards, for SAO terpolymers as macroinitiators with initial molar feed compositions a)  $f_{STY,0} = 0.40$ ,  $f_{AN,0} = 0.50$ ,  $f_{iPOx} = 0.10$ , b)  $f_{STY,0} = 0.50$ ,  $f_{AN,0} = 0.30$ ,  $f_{iPOx} = 0.20$ 

The leftward shifting of the peaks with time, toward smaller elution time shows that the chains are growing since longer chains elute from the column faster than smaller chains in GPC.

## 3.3.4. Thermal Properties of SAO polymer

Table 19. Thermal properties of SAO via NMP

Polymer	M	lole Fract polymer		GlassTransition Temperature $T_g(^{\circ}C)$	Decomposition Temperature (°C)	M <sub>n</sub> (g/mol)
	STY	AN	iPOx	Ig(C)	( 0)	(g/IIIOI)
SAO	0.13	0.83	0.03	85	200	9,300
SAO	0.18	0.75	0.07	90	200	3,500
SAO	0.45	0.27	0.28	70	200	19,500

The decomposition temperature of the SAO polymer was 200 °C. Therefore, the solvent casting had to be done at temperatures below 200 °C but above 100 °C to ensure that the SAO melts and can be reacted with the PE – AA. The glass transition ( $T_g$ ) values were dependent on the feed ratio of monomers. The  $T_g$  of poly(styrene) in literature was around 100 °C [47] and poly(acrylonitrile) was 85 °C [48] but these were only mean values since the  $T_g$  depends on many factors (including molecular weight, cross linking and rate of cooling) [49]. **Table 19** shows that when the amount of acrylonitrile dominated the polymer composition ( $F_{AN} = 0.83$ ), the  $T_g$  value (85 °C) corresponded to that of poly(acrylonitrile) in literature but when the amount of styrene in the polymer increased ( $F_{STY} = 0.18$ ), the  $T_g$  value also increased (90 °C) since poly(styrene) had a higher  $T_g$  value in literature. However, the amount of 2-isopropyl-2-oxazoline in the polymer also influences the  $T_g$ . When a larger amount of iPOx was present ( $F_{iPOx} = 0.28$ ), the  $T_g$  of the copolymer corresponded with that of poly(2-isopropyl-2-oxazoline) in literature (70 °C) [50].

## 3.3.5. Solvent casting of SAO and Acrylic acid Grafted Poly(ethylene)

Oxazoline derivatives have been shown to be highly reactive toward a number of functional groups, including carboxyl acids [43]. Oxazoline functional groups have previously been added as compatibilizers to blends and shown to improve blending properties and processability of ethylene–acrylic acids (EAA), poly amides (PA) and low density polyethylene (LDPE) blends [44]. In this study, an oxazoline functional copolymer of styrene and acrylonitrile (SAO) was

reacted with acrylic acid grafted poly(ethylene) (PE - AA). The reaction shown in **Figure 27** was expected to take place [43].

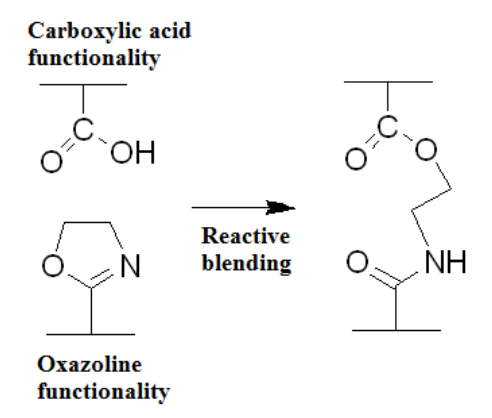


**Figure 27.** Reactive blending of Oxazoline and Carboxylic acid
The microstructure of the blends was characterized using SEM analysis (**Figure 28**).

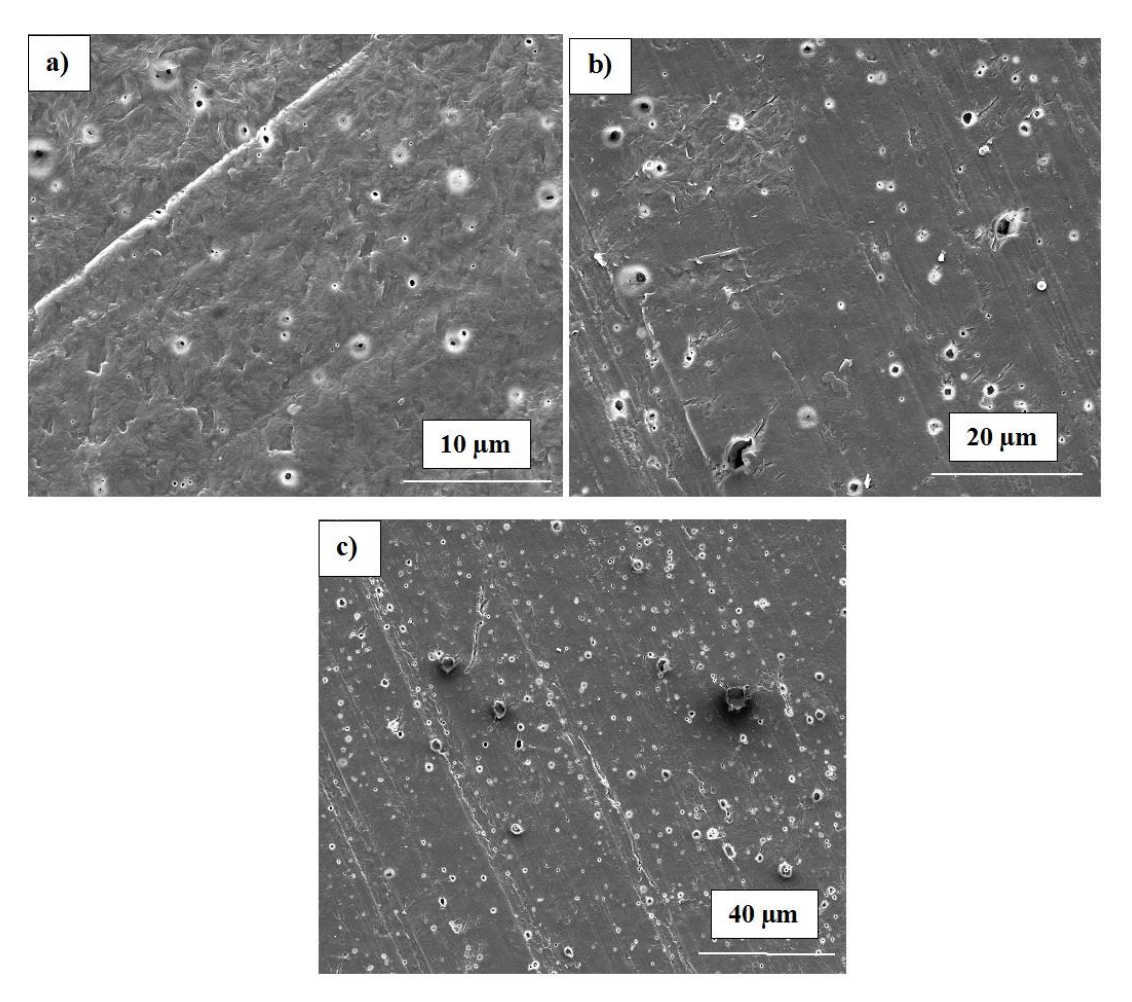


Figure 28. SEM images of PE – AA /SAO (80/20), annealed at 130 °C for 6 hours

The images shown are not representative of what an 80 wt% PE – AA and 20 wt% SAO blended ratio should look like. This observation was based on the fact that the concentration of the particles is low. The images shown in **Figure 28** do not show a 20% dispersed phase in surface area. This may be due to the incomplete dissolution of PE in the toluene during solvent casting, which may affect the final blend composition. This means that there may not have been 80 wt% PE – AA in the solution hence, the entire material was not able to react with the oxazoline functionality to form a blend. The characterization of the images is shown in **Table 20**.

Table 20. Summary of blend microstructure for extruded blends and annealed blends

Terpolymer	Polymer feed ratio	Blend Ratio by Wt%	Etching Time (h)	Annealing Conditions (°C)	<b>⟨D⟩</b> <sub>VS</sub> (μm)	Number of Particles
SAO	50:20:30	80:20	2	120	1.42	314

## 3.4. Conclusion

In conclusion, the NMP synthesis of Sty-AN-Ox (SAO) was controlled, as a significantly high conversion ( $\sim 60$  % molar conversion) with low PDI ( $M_w/M_n$ ) of around 1.3 could be achieved. There was also evidence suggesting that the polymers were formed in a controlled manner with active chain ends, which means that the terpolymer can be chain extended using other monomers to add additional properties to the terpolymer and tailor it to the needs of the industry/application.

### 3.5. Future Work

The next step would be blending the polymer with PE using extrusion techniques instead of solvent casting. However, the SAO polymer needs to be extruded at temperatures greater than 112 °C whereas, this particular grade of PE – AA, processing temperatures above 100 °C were too high and did not produce mechanically strong blends. Therefore, PE – AA requires operating

temperatures between  $90-100\,^{\circ}\text{C}$  for extrusion. Hence, solvent casting was used for this particular grade of PE – AA.

#### **GENERAL CONCLUSION**

The work carried out in this thesis showed initial steps toward the developing barrier materials tailored to the needs of the industry through reactive blending with functional poly(ethylene). It was shown that a primary amine monomer (IDBA) can be synthesized in large quantities and polymerized by conventional radical polymerization to form an amine functional polymer (MA/AN/IDBA) which can then be melt blended with maleic anhydride grafted PE (PE-MAn) in a miniature twin screw extruder at a level of 20 wt.% MA/AN/IDBA and 80 wt.% PE-MAn and shown to form a compatible blend when compared to blends made with non-functional MA/AN/AMS and PE-MAn. The finer particle dispersion obtained with the amine functional blend showed that dynamic coalescence was prevented by the formation of covalent bonds formed between the functional polymers.

It was also shown that in a similar manner, functional groups other than amine and anhydride can also be reacted to form functional blends. Oxazoline functional terpolymers were synthesized (STY/AN/iPOx) and blended with acrylic acid grafted poly(ethylene) (PE – AA) using solvent casting. The results did not allow an accurate conclusion to be derived due to insufficient mixing and drawbacks associated with the solvent casting method. The next steps in this project would be to melt blend oxazoline functional terpolymers with a different grade of PE – AA (more thermally stable) using extrusion.

### REFERENCES

- 1. DeLassus, P., Barrier Polymers, in Kirk-Othmer Encyclopedia of Chemical Technology. 2000, John Wiley & Sons, Inc.
- 2. Robert J. Young, P.A.L., Introduction to Polymers. Third ed. 2011: CRC Press.
- 3. Braunecker, W.A. and K. Matyjaszewski, Controlled/living radical polymerization: Features, developments, and perspectives. Progress in Polymer Science, 2007. 32(1): p. 93-146.
- 4. Hawker, C.J., A.W. Bosman, and E. Harth, New Polymer Synthesis by Nitroxide Mediated Living Radical Polymerizations. Chemical Reviews, 2001. 101(12): p. 3661-3688.
- 5. Sadiku-Agboola, O., et al., Rheological properties of polymers: structure and morphology of molten polymer blends. Materials Sciences and Applications, 2011. 2(01): p. 30.
- 6. Utracki, L.A., Compatibilization of Polymer Blends. The Canadian Journal of Chemical Engineering, 2002. 80(6): p. 1008-1016.
- 7. Summers, G.J., M.P. Ndawuni, and C.A. Summers, Primary amine functionalized polystyrenes by atom transfer radical polymerization. Polymer International, 2003. 52(1): p. 158-163.
- 8. Marić, M., et al., Incorporating primary amine pendant groups into copolymers via nitroxide mediated polymerization. Reactive and Functional Polymers, 2011. 71(12): p. 1137-1147.
- 9. Liu, N.C. and W.E. Baker, Reactive polymers for blend compatibilization. Advances in Polymer Technology, 1992. 11(4): p. 249-262.
- 10. Wu, M.M., Acrylonitrile and Acrylonitrile Polymers, in Encyclopedia of Polymer Science and Technology. 2002, John Wiley & Sons, Inc.
- 11. Yang Zhenghua, Y.L., Barrier Property and Structure of Acrylonitrile/Acrylic copolymers. Chinese Journal of Polymer Science, 1997. 15(3): p. 236 241.
- 12. Zhenghua, Y., Yuesheng Li, Barrier property and structure of acrylonitrile/acrylic copolymers. Chinese Journal of Polymer Science, 1997. 15(3): p. 236 241.
- 13. The Wiley Encyclopedia of Packaging Technology. Third ed.: John Wiley & Sons, Inc.
- 14. Kratofil, L.J., et al., Compatibilization Effects in SAN/EPDM Blends Prepared by Reactive Extrusion. Journal of Elastomers and Plastics, 2007. 39(4): p. 371-382.
- 15. Sigma Aldrich. 536180 ALDRICH 4-Vinylaniline. Available from: <a href="http://www.sigmaaldrich.com/catalog/product/aldrich/536180?lang=en&region=CA">http://www.sigmaaldrich.com/catalog/product/aldrich/536180?lang=en&region=CA</a> [Accessed 25 November 2015].
- 16. Sigma Aldrich. 15369 ALDRICH N-Boc-ethylenediamine. Available from: <a href="http://www.sigmaaldrich.com/catalog/product/aldrich/15369?lang=en&region=CA">http://www.sigmaaldrich.com/catalog/product/aldrich/15369?lang=en&region=CA</a> [Accessed 25 November 2015].

- 17. D.L. Trumbo, B.E.M., A.S. Trevino, M. Van Den Brink, Copolymerization Behavior of 3-Isopropenyl-α,α–Dimethylbenzylamine and a Preliminary Evaluation of the Copolymers in Thermoset Coatings. Journal of Applied Polymer Science, 2001. 82: p. 1030 1039.
- 18. Sigma Aldrich. 361771 ALDRICH 3-Isopropenyl-α,α-dimethylbenzyl isocyanate. Available from:
- http://www.sigmaaldrich.com/catalog/product/aldrich/361771?lang=en&region=CA [Accessed 25 November 2015].
- 19. Odian, G., Principles of Polymerization, Chapter 6. 4th ed. 2004: John Wiley & Sons, Inc.
- 20. Tüdos, F., et al., Analysis of the linear methods for determining copolymerization reactivity ratios. VI. A comprehensive critical reexamination of oxonium ion copolymerizations. Journal of Polymer Science: Polymer Chemistry Edition, 1981. 19(5): p. 1119-1132.
- 21. Nevin, Ç., M. Mursit Temuz, Characterization and monomer reactivity ratios of grafted cellulose with N-(4-nitrophenyl)acrylamide and methyl methacrylate by atom transfer radical polymerization. Cellulose Chem. Technol., 2012. 46(9 10): p. 551 558.
- 22. F Ziaee. M Nekoomanesh, Monomer reactivity ratios of styrene-butyl acrylate copolymers at low and high conversions Polymer, 1997. 39(1): p. 203 207.
- 23. Mayo, F.R. and F.M. Lewis, Copolymerization. I. A Basis for Comparing the Behavior of Monomers in Copolymerization; The Copolymerization of Styrene and Methyl Methacrylate. Journal of the American Chemical Society, 1944. 66(9): p. 1594-1601.
- 24. Wiles, K.B., et al., Monomer reactivity ratios for acrylonitrile—methyl acrylate free-radical copolymerization. Journal of Polymer Science Part A: Polymer Chemistry, 2004. 42(12): p. 2994-3001.
- 25. J. Vinas, N.C., D. Gigmes, T. Trimaille, A. Favier, D. Bertin, SG1-based alkoxyamine bearing a N-succinimidyl ester: A versatile tool for advanced polymer synthesis. Polymer, 2008. 49: p. 3639 3647.
- 26. Charles, F.K.I.I., G.J. McCollum, and C.A. Wilson, Preparation of alkyl primary amines. US4927969 A. 1990, Google Patents.
- 27. Personal Reaction Station Manual, I. J-KEM Scientific, Editor.
- 28. Marić, M. and C.W. Macosko, Improving polymer blend dispersion in mini-mixers. Polymer Engineering & Science, 2001. 41(1): p. 118-130.
- 29. Marić, M. and C.W. Macosko, Block copolymer compatibilizers for polystyrene/poly(dimethylsiloxane) blends. Journal of Polymer Science Part B: Polymer Physics, 2002. 40(4): p. 346-357.
- 30. V.A. Bhanu, P.R., K. Wiles, M. Bortner, M. Sankarpandian, D. Godshall, T.E. Glass, A.K. Banthia, J. Yang, G. Wilkes, D. Baird, J.E. McGrath, Synthesis and characterization of

- acrylonitrile methyl acrylate statistical copolymers as melt processable carbon fiber precursors. Polymer, 2002. 43: p. 4841 4850.
- 31. Zengeni, E., et al., Poly(acrylonitrile-co-methyl acrylate) copolymers: Correlation between copolymer composition, morphology and positron annihilation lifetime parameters. Journal of Applied Polymer Science, 2011. 119(2): p. 1060-1066.
- 32. Tüdos, F., et al., Analysis of Linear Methods for Determining Copolymerization Reactivity Ratios. III. Linear Graphic Method for Evaluating Data Obtained at High Conversion Levels. Journal of Macromolecular Science: Part A Chemistry, 1976. 10(8): p. 1513-1540.
- 33. Subramanian, P.M., Permeability barriers by controlled morphology of polymer blends. Polymer Engineering & Science, 1985. 25(8): p. 483-487.
- 34. Oxby, K.J. and M. Marić, Compatibilization of Poly(styrene-acrylonitrile) (SAN)/Poly(ethylene) Blends via Amine Functionalization of SAN Chain Ends. Macromolecular Reaction Engineering, 2014. 8(2): p. 160-169.
- 35. H.K. Jeon, C.W.M., B. Moon, and T.R. Hoye,, Coupling reactions of end- vs. mid-functional polymers. Macromolecules, 2004. 37: p. 2563-2571.
- 36. Ashcraft, E., et al., A Novel Reactive Processing Technique: Using Telechelic Polymers To Reactively Compatibilize Polymer Blends. ACS Applied Materials & Interfaces, 2009. 1(10): p. 2163-2173.
- 37. Salame, M. and S. Steingiser, Barrier Polymers. Polymer-Plastics Technology and Engineering, 1977. 8(2): p. 155-175.
- 38. Vinas, J., et al., SG1-based alkoxyamine bearing a N-succinimidyl ester: A versatile tool for advanced polymer synthesis. Polymer, 2008. 49(17): p. 3639-3647.
- 39. Zhang, C. and M. Maric, Synthesis of Stimuli-responsive, Water-soluble Poly[2-(dimethylamino)ethyl methacrylate/styrene] Statistical Copolymers by Nitroxide Mediated Polymerization. Polymers, 2011. 3(3): p. 1398.
- 40. Nicolas, J., S. Brusseau, and B. Charleux, A minimal amount of acrylonitrile turns the nitroxide-mediated polymerization of methyl methacrylate into an almost ideal controlled/living system. Journal of Polymer Science Part A: Polymer Chemistry, 2010. 48(1): p. 34-47.
- 41. Weber, C., et al., 2-Isopropenyl-2-oxazoline: A Versatile Monomer for Functionalization of Polymers Obtained via RAFT. Macromolecules, 2012. 45(1): p. 20-27.
- 42. Szwarc, M., Living polymers. Their discovery, characterization, and properties. Journal of Polymer Science Part A: Polymer Chemistry, 1998. 36(1): p. IX-XV.
- 43. Frump, J.A., Oxazolines. Their preparation, reactions, and applications. Chemical Reviews, 1971. 71(5): p. 483-505.
- 44. Wei, Q., D. Chionna, and M. Pracella, Reactive Compatibilization of PA6/LDPE Blends with Glycidyl Methacrylate Functionalized Polyolefins. Macromolecular Chemistry and Physics, 2005. 206(7): p. 777-786.

- 45. McManus, N.T., A. Penlidis, and M.A. Dube, Copolymerization of alpha-methyl styrene with butyl acrylate in bulk. Polymer, 2002. 43(5): p. 1607-1614.
- 46. Martinet, F. and J. Guillot, Copolymerization with depropagation: Experiments and prediction of kinetics and properties of  $\alpha$ -methylstyrene/methyl methacrylate copolymers. I. Solution copolymerization. Journal of Applied Polymer Science, 1997. 65(12): p. 2297-2313.
- 47. Rieger, J., The glass transition temperature of polystyrene. Journal of thermal analysis, 1996. 46(3): p. 965-972.
- 48. Sigma Aldrich, 181315 ALDRICH Polyacrylonitrile. Available from: <a href="http://www.sigmaaldrich.com/catalog/product/aldrich/181315?lang=en&region=CA">http://www.sigmaaldrich.com/catalog/product/aldrich/181315?lang=en&region=CA</a> [Accessed 27 March 2016].
- 49. UK Essays. Polymer The Glass Transition, 2013. Available from: <a href="https://www.ukessays.com/essays/chemistry/polymer-the-glass-transition.php?cref=1">https://www.ukessays.com/essays/chemistry/polymer-the-glass-transition.php?cref=1</a> [Accessed 27 March 2016].
- 50. Oleszko, N., et al., Crystallization of Poly(2-isopropyl-2-oxazoline) in Organic Solutions. Macromolecules, 2015. 48(6): p. 1852-1859.